Analysis of the Steady State Performance of Doubly Fed Induction Generator

Thesis submitted in partial fulfillment of the requirements for the award of the degree of

MASTER OF ENGINEERING
in
POWER SYSTEMS & ELECTRIC DRIVES

Submitted By
Manu Sharma
(Roll No. 801041014)

Under the supervision of:

Dr. Sanjay K. Jain
Associate Professor, EIED

ELECTRICAL & INSTRUMENTATION ENGINEERING DEPARTMENT
Thapar University
Patiala-147004

JULY-2012

CERTIFICATE

I hereby declare that the Thesis entitled **"Analysis of the Steady State performance of Doubly Fed Induction Generator"** is an authentic record of my own work carried out as the requirements for the award of the degree of M.E. (Power Systems & Electric Drives) at Thapar University, Patiala, under the guidance of **Dr. Sanjay K. Jain**, Associate Professor, EIED.

The matter presented in this Thesis has not been submitted for the award of any other degree of this or any other university.

Manu Sharma
13/7/12

Manu Sharma
(Regn. no.-801041014)

It is certified that the above statement made by the student is correct to the best of my knowledge and belief.

Sanjay 13/07/2012

Dr. Sanjay K. Jain
Associate Professor

Countersigned by:

S. Ghosh

Dr. Smarajit Ghosh
Professor & Head,EIED
Thapar University, Patiala

Dr. S.K. Mohapatra
Dean, Academic Affairs
Thapar University, Patiala

i

ACKNOWLEDGEMENT

I would like to express my sincere gratitude to my supervisor, **Dr. Sanjay K. Jain, Associate Professor (EIED),** for all his guidance and invaluable advises throughout the progress. He has stimulated my interest in power engineering and inspired me for doing research on this topic.

I would also like to thank **Dr. Smarajit Ghosh,** Professor & Head, Electrical & Instrumentation Engineering Department (EIED) and **Mrs. Manbir Kaur**, Associate Professor & P.G. Coordinator (PSED) for extending all the needed help to carry out this work.

I would like to thank my family and all my friends for their continuous support and encouragement.

Manu Sharma

(Regn. No. 801041014)

ABSTRACT

In recent years, wind power is proved to be the most reliable and developed renewable energy source. The share of wind power with respect to total installed power capacity is increasing worldwide. The evolution of technology related to wind systems leads to the development of a generation of variable speed wind turbines that present many advantages compared to the fixed speed wind turbines. The system studied here is a variable speed wind generation system Doubly Fed Induction Generator (DFIG). The DFIG is one of the popular wind power generator in the wind power industry. The stator of the generator is directly connected to the grid while the rotor is connected through an AC/DC/AC back-to-back PWM converter.

In this thesis the steady state performance of DFIG is analyzed. The DFIG is assumed to be connected in power system. The DFIG is modeled as PQ bus for arising the AC system solution. With the help of converged power flow solution, the steady state performance is calculated using Newton Raphson method. Steady state performance of the DFIG is analyzed for its operation at leading power factor, lagging power factor and unity power factor.

TABLE OF CONTENTS

LIST OF FIGURES

LIST OF TABELS

CHAPTER-1

INTRODUCTION

1.1 OVERVIEW

Wind energy is a relatively young but rapidly expanding industry. Wind energy is an intermittent resource as we get electricity only when the wind blows. Although modern wind turbines regulate power well and level off at their rated capacity, the amount of power they produce varies throughout the day. Hundreds of installations have demonstrated that utility systems are capable of accommodating the changing wind power just as they modify their output to follow changing demand. Experts predict that wind power can compose up to 30% of our energy mix before reliability of the system would be an issue.

Wind Energy is generated by harnessing the kinetic energy of atmospheric air. It has had been in use for centuries for several other purposes such as sailing, irrigation and for grinding grain. Wind power systems transform kinetic energy of the wind into useful sources of power. During ancient times, wind power systems were used for both milling and irrigation. It was during the early years of the 20th century that wind power was started to be harnessed for generation of electricity. Windmills have also been used in several countries to pump water.

Wind turbines work by transforming the Wind Energy into mechanical power that can be used for conversion to electricity or for other mechanical purposes like grinding. Wind turbines are used either as stand-alone units or in groups known as Wind Farms. Small-sized wind turbines, known as aero generators are used for charging large-sized batteries.

More than 80% of the global Wind Energy capacity is installed in 5 countries with India at the 5th position. Wind power is the fastest growing source of renewable energy globally with an increasing capacity every year.

Harnessing wind energy for electric power generation is an area of research interest and at present, the emphasis is given to the cost effective utilization of energy resources for quality and reliable power supply. Among various techniques, the use of the doubly fed induction generator appeared to be good solution for such application. The induction

generator is favored for wind power plants because of its simplicity, robustness and small size per generator kW, lower maintenance and ease of control.

1.2 LITERATURE REVIEW

Many investigations have been made in the field of wind power generation over the past few decades. These investigation deals with behavior, modeling, speed control of doubly fed induction generator. Wind turbines models in the load flow analysis have been discussed in many works. The brief literature is summarized here.

Polinder and Kling (2001) [1] generated electricity from renewable wind sources using wind turbines. A dynamic model of contemporary wind turbine concept was presented. This was regarded as doubly fed (wound rotor) induction generator with a voltage source converter in the rotor. This wind turbine concept is equipped with rotor speed, pitch angle and terminal voltage controllers.

Fernando *et al*. (2010) [24] conducted an analysis of steady-state operation of wind turbine driven doubly-fed induction generator (DFIG). A method based on the Newton-Raphson (NR) algorithm is proposed for obtaining the steady-state electrical variables of the machine under certain given conditions. It is of interest in the load flow analysis and for gaining initial conditions for dynamic analysis.

Mustafa *et al.* (2005) [2] studied the wind power market. It is observed that the DFIG is an ideal candidate to satisfy the requirements of the recently proposed challenging grid codes. The attempt is made to clarify the existing ambiguities in modeling of DFIG under various operating conditions. The DFIG model utilizing the current controllers for the rotor-side and grid-side converter is presented.

Liu *et al.* (2008) [6] studied existing wind farm models in power flow calculation. The power flow algorithms for power system including wind farm consisting of squirrel cage induction generators (SCIG) or doubly-fed induction generators (DFIG) are developed. Since reactive power of wind farm is rectified synchronously in every power flow iterative process, the improved algorithms avoid additional calculations, hold low-computational costs and respectively and reflect the two kinds of wind farms characteristics accurately.

Holdsworth and Ekanayake (2004) [3] addressed the issue of large wind farms based on doubly fed induction generator (DFIG) being integrated into power system. The

dynamic model, which can be used to simulate the DFIG wind turbine using a single-cage and double-cage representation of the generator rotor, as well as a representation of its control and protection circuits is presented. The model is suitable for use in transient stability programs that can be used to investigate large power systems. The behavior of a wind farm and the network under various system disturbances was studied using this dynamic model. The influence of the DFIG control on the stability of the wind farm was also investigated by considering different control gains and by applying network voltage control through both stator side and rotor side converters.

Salman and Badrzade (2002) [4] observed the penetration of wind power into electrical grids. They presented simulation results of a Grid connected DFIG. A switch-by-switch representation of the PWM converters with a carrier-based Sinusoidal PWM modulation for both rotor- and stator-side converters has been presented. Stator-Flux Oriented vector control approach is deployed for both stator- and rotor-side converters to provide independent control of active and reactive power and keep the DC-link voltage constant.

Cheng *et al.* (2009) [5] reviewed three typical variable speed wind turbine concepts, including multi-stage doubly-fed induction generator (DFIG), direct-drive electrical excited synchronous generator (EESG) and direct drive permanent magnet synchronous generator (PMSG).

Lei *et al.* (2006) [6] highlighted the advantages such as the improved power quality, high energy efficiency and controllability, etc. of the variable speed wind turbine using a doubly fed induction generator (DFIG). They developed a simple DFIG wind turbine model in which the power converter is simulated as a controlled voltage source, regulating the rotor current to meet the command of real and reactive power production. Their model has the form of traditional generator model and hence can be integrated into the power system easily.

1.3 MOTIVATION OF THE RESEARCH

Wind power is the most reliable and developed renewable energy source over past decades. The increased awareness of people towards renewable energy, support from governmental institution, and rapid advancement in the power electronics industry, which is the core of wind power systems, are the most contributing factors for the development of wind power systems. As a result, the share of wind power with respect to total installed

power capacity is increasing worldwide. The WECS utilizing variable-speed variable-pitch wind turbine with DFIG is the most popular in the wind power industry especially for multi-megawatt size. The beauty of the DFIG-based WECS is its efficient power conversion capability at variable wind speed with reduced mechanical stress and low price because of partial size rated power converters needed to achieve the full control of the machine. These favorable technical and economical characteristics have encouraged the commercialization of this wind turbine in the modern wind power industry quickly. Unfortunately, these kinds of wind turbine have limited reactive power capability and are typically connected at remote areas and offshore mainly because of favorable wind condition, noise pollution, physical dimension and impact on the scenery. Hence, to assist its future integration into the modern power system, it is therefore important to access its performance.

1.4 OBJECTIVES OF THE THESIS

The thesis work has been carried out with the main objective to analyze the steady state study performance of wind driven grid connected doubly fed induction generator. The DFIG is assumed to be the part of power system for realistic behavior.

1.5 ORGANIZATION OF THE THESIS

The work carried out in this thesis has been summarized into four chapters. The **Chapter-1** summarizes the overview of thesis, literature review, and motivation of research, objective of thesis work and objective of thesis work. The **Chapter-2** describes wind energy scenario and various aspects of wind power generation system. The **Chapter-3** summarizes operating principle DFIG and the steady state analysis of DFIG algorithm to calculate steady state performance is also presented. The **Chapter-4** presents the results obtained from presented algorithm. The conclusion and scope of future work are detailed in **Chapter-5.**

CHAPTER-2

2.1 WIND ENERGY

Wind energy is energy collected from motion caused by heavy winds. Wind energy is collected in turbines with propellers that spin when the wind blows and turn the motion of the propeller into energy that can be used in the electrical grid. Wind energy is a clean, renewable energy source that is abundant in windy areas. Large wind farms are often located outside of cities, supplying power for electrical grids within the city. Wind turbines come in a variety of sizes that can be used to supply power to individual buildings or feed electricity into a grid system. They must be located above nearby buildings and trees to work effectively for a home or building. Considerations to be taken when installing a wind turbine include location, average wind speed, the height of the surrounding buildings and trees, and the building's connection to the electrical grid.

2.2 THE GLOBAL SCENARIO OF WIND POWER

The expectations for wind power market growth in 2010 were mixed, as the low level of orders seen during the financial crisis worked their way through the system. The results of this were felt much more strongly in 2010 than in the previous year, and the overall annual market shrunk by 0.5% to 38.3 GW, down from 38.8 GW in 2009. The new capacity added in 2010 represents investments worth EUR 49.8 billion (USD 71.8 billion). Despite the decrease in annual installations, global installed wind power capacity increased by 24.1% during the year, and now stands at 197.0 GW. For most other sectors that have not become accustomed to growth rates of 30% or more, this would represent a major achievement.[12]

For the first time in 2010, more than half of all new wind power was added outside of the traditional markets of Europe and North America. This was mainly driven by the continuing boom in China, which accounted for half the new global wind installations, with 18.9 GW. China now has 44.7 GW of wind power, and has surpassed the US to claim the number in terms of total installed capacity.

The US market installed almost 50% less than in 2009. In the European market, new installed capacity in 2010 was 7.5% down on 2009, despite a 50% growth of the offshore market in countries like the UK, Denmark and Belgium, and rapid growth in Eastern Europe, led by Romania, Bulgaria and Poland.

2.2.1 TOP TEN CUMMULATIVE CAPACITY OF WIND ENERGY

Table 2.1 Top ten cumulative capacities by year 2010 [12]

COUNTRY	MW	%
China	44,733	22.7
USA	40,180	20.4
Germany	27,214	13.8
Spain	20,676	10.5
India	13,065	6.6
Italy	5,797	2.9
France	5,660	2.9
UK	5,204	2.6
Canada	4,009	2.0
Denmark	3,752	1.9
Rest of the world	26,749	13.6
TOTAL	**197,039**	**100**

2.3 STATUS OF WIND POWER IN INDIA

According to the Ministry of New and Renewable Energy (MNRE), today the share of renewable based capacity is 10.9% (excluding large hydro) of the total installed capacity of 170 GW in the country, up from 2% at the start of the 10th Plan Period (2002-2007). This includes 13,065.78 MW of wind, 2,939 MW of small hydro power, 1,562 MW of cogeneration, 997 MW of biomass, 73.46 MW of 'waste to power' and 17.80 MW of solar photovoltaic for grid connected renewable at the end of 2010.

India had a record year for new wind energy installations in 2010, with 2,139 MW of new capacity added to reach a total of 13,065 MW at the end of the year. Renewable energy is now 10.9% of installed capacity, contributing about 4.13% to the electricity generation mix, and wind power accounts for70% of this installed capacity. Currently the wind power potential estimated by the Centre for Wind Energy Technology (C-WET) is 49.1 GW, but the estimations of various industry associations and the World Institute for Sustainable Energy (WISE) and wind power producers are more optimistic, citing a potential in the range of 65-100 GW. Historically, actual power generation capacity additions in the conventional power

sector in India have been fallen significantly short of government targets. For the renewable energy sector, the opposite has been true, and it has shown a tendency towards exceeding the targets set in the five-year plans. This is largely due to the booming wind power sector.

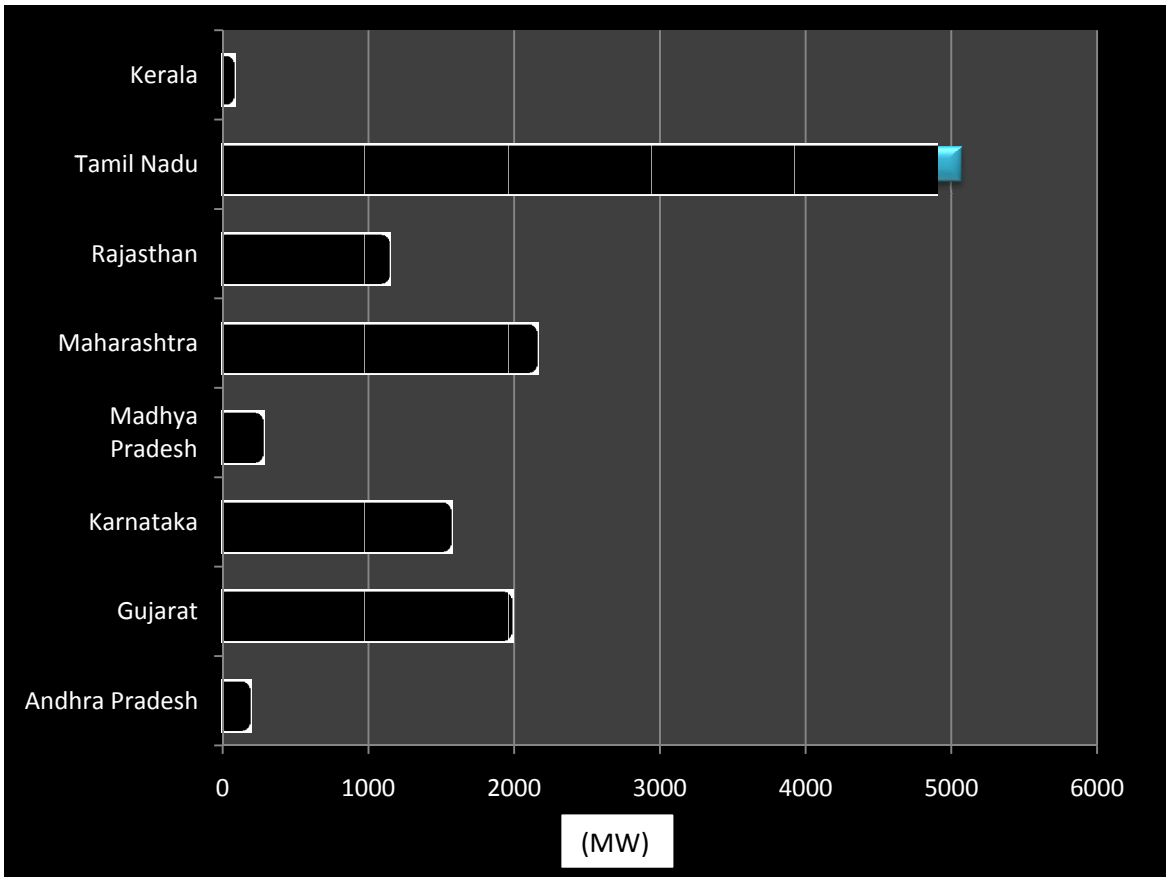

Figure 2.1 State wise generation and installed capacity in (MW)

Table 2.2 State wise generation and installed capacity in (MW)

STATE	CAPACITY (MW)

ANDHRA PRADESH	138.40
GUJARAT	1,934.60
KARNATAKA	1,517.20
MADHYA PRADESH	230.80
MAHARAHTRA	2,108.10
RAJASTHAN	1,095.60
TAMIL NADU	5,073.10
KERALA	28.00
TOTAL	**12,125.80**

2.4 INTRODUCTION TO WIND ENERGY CONVERSION SYSTEM

Wind Energy Conversion System (WECS) is the overall system for converting wind energy into useful mechanical energy that can be used to power an electrical generator for generating electricity. The WECS basically consists of three types of components: aerodynamics, mechanical, and electrical as shown in figure 2.2. [8]

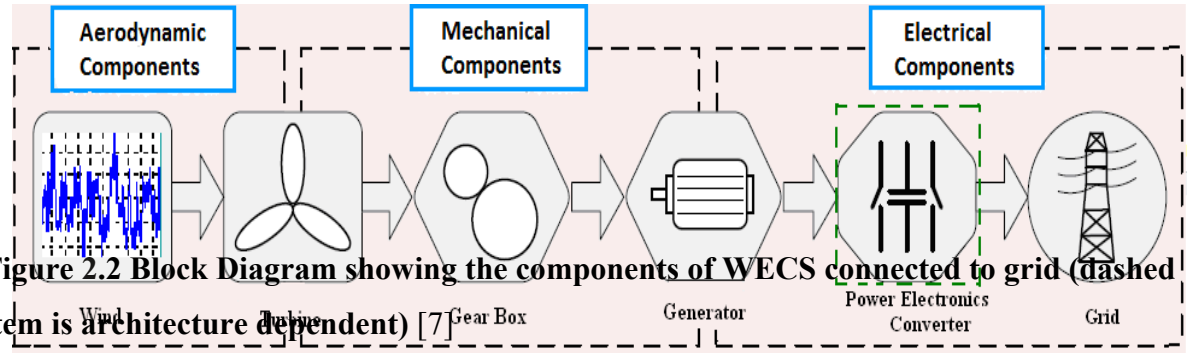

Figure 2.2 Block Diagram showing the components of WECS connected to grid (dashed item is architecture dependent) [7]

2.4.1 WIND TURBINES

I .VAWT/HAWT

From the physical setup viewpoint, there are horizontal axis wind turbines (HAWT) and vertical axis wind turbines (VAWT) as shown in figure 2.3 and 2.4.[7]Initially, vertical axis designs were considered due to their expected advantages of omni-directionality (hence do not need yaw-system) and having gears and generating equipments at the tower base. However, the following disadvantages caused the VAWT to have a diminished presence in the commercial market:

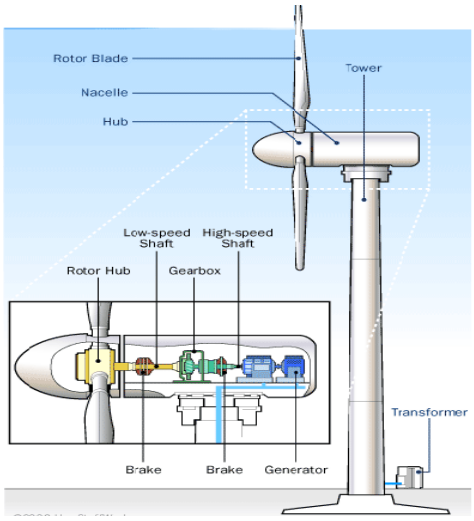

Figure 2.3 Vertical axis wind turbine.

- Reduced aerodynamic efficiency: much of the blade surface is close to the axis.
- Housing usually at ground level so it is not feasible to have the gearbox of large VAWT at ground level because of the weight and cost of the transmission shaft.

In HAWT, the wind turbine blades rotate about an axis parallel to the ground and wind flow. Almost all the larger turbines employed in modern wind farms are HAWT because they are more suitable for harnessing more wind energy. However, HAWT are subjected to reversing gravitational loads (structural load is reversed when the blade goes from upwards to downwards position) which impose a limit on the size of such turbines. The rotation of both HAWT and VAWT can be powered primarily by lift or drag force depending on the design of the blade.

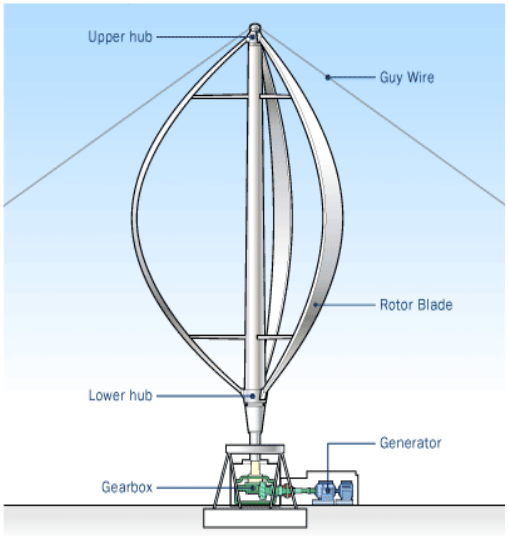

Figure 2.4 Horizontal axis wind turbine

II. Variable-speed, Pitch-regulated Wind Turbine

A variable speed wind turbine can incorporate a pitch regulation feature that involves turning the blades about their lengthwise axes (pitching the blades) to regulate the power extracted by the rotor.

Advantages:

- Turbine can operate at ideal tip-speed ratios over a larger range of wind speeds so as to capture maximum energy from wind.
- Ability to supply power at a constant voltage and frequency while the rotor speed varies.
- Control of the active and reactive power.

Disadvantages:

- Generates variable frequency current/voltage so needs power electronic converter.

III. Fixed-speed, Stall-regulated Wind Turbine

When the wind speed increases, the blades become increasingly stalled to limit power to acceptable levels without any additional active control hence the rotor speed is held essentially constant.

Advantages:

- Simple and robust construction, hence lower capital cost.

Disadvantages:

- Cannot extract optimum energy from wind.

2.4.2 COMPONENTS OF WIND TURBINES

The major components of a wind turbine system are shown in figure 1.3 (drawing not to scale). The turbine is formed by the blades, the rotor hub and the connecting components. The drive train is formed by the turbine rotating mass, low-speed shaft, gearbox, high-speed shaft, and generator rotating mass. It transfers turbine mechanical output power up to the generator rotor where it is converted to electrical power. The wind strikes the rotor on the horizontal-axis turbine, causing it to spin. The low-speed shaft transfers energy to the gear box, which steps up in speed and rotates the high speed shaft. The high speed shaft causes the generator to spin, hence generating electricity. The yaw system is used to turn the nacelle so that the rotor faces into the wind. The low speed shaft contains pipes for the hydraulics system that operates the aerodynamic brake. The high speed shaft is equipped with an emergency mechanical brake which is used in case of failure of the aerodynamic brake.

The generator converts mechanical power of wind into electrical power. Usually the generator produces power at low voltage and the transformer steps up the generator output voltage to connected grid voltage. The transformer may be placed at the bottom of the tower or in the nacelle for losses minimization.

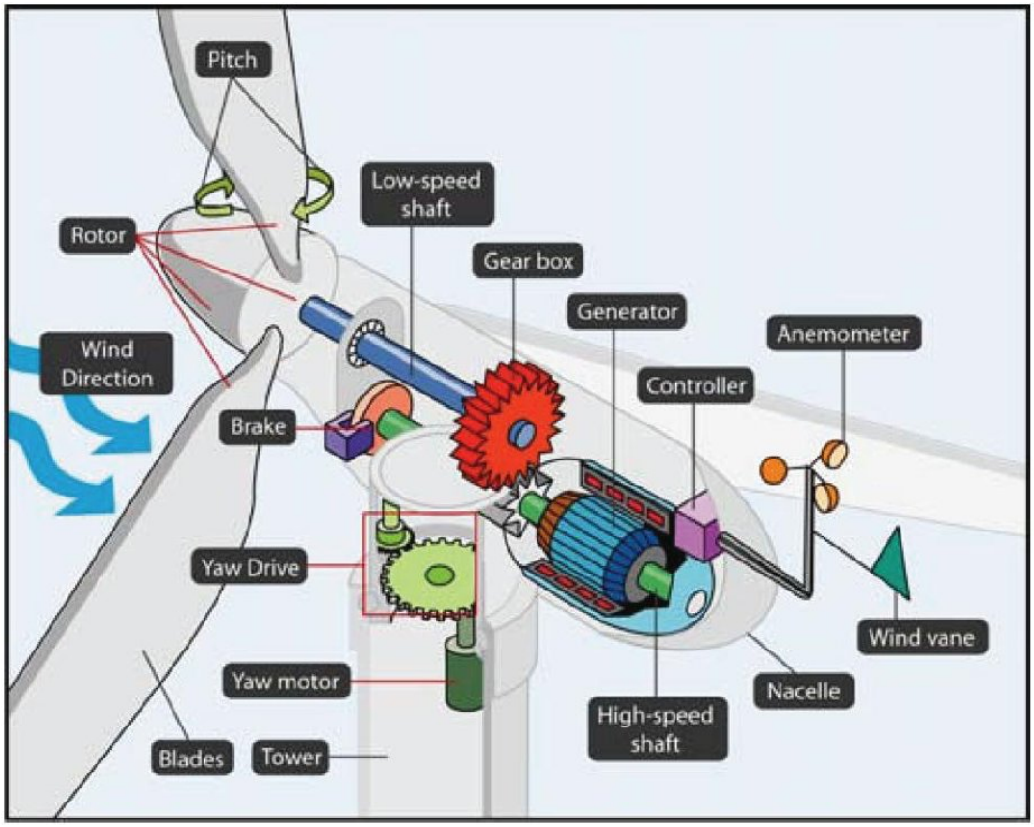

Figure 2.5 HAWT showing mechanical, electrical, and control components [11]

Other components of wind turbine system are the anemometer to measure wind speed and a wind vane which measure the wind direction. Wind speed information is used to determine when the wind speed is sufficient to start up the turbine and when, due to high winds, the turbine must be shut down for safety whereas wind direction measurement is used by the yaw-control mechanism which helps in orienting the rotor to the wind direction. Electric fans and oil coolers are used to cool the gearbox and generator.[11]

2.4.3 OPERATING REGION OF THE WIND TURBINE

The operating region of a variable-speed variable-pitch wind turbine can be illustrated by their power curve, which gives the estimated power output as function of wind speed as shown in figure 2.6. Three distinct wind speed points can be noticed in this power curve:

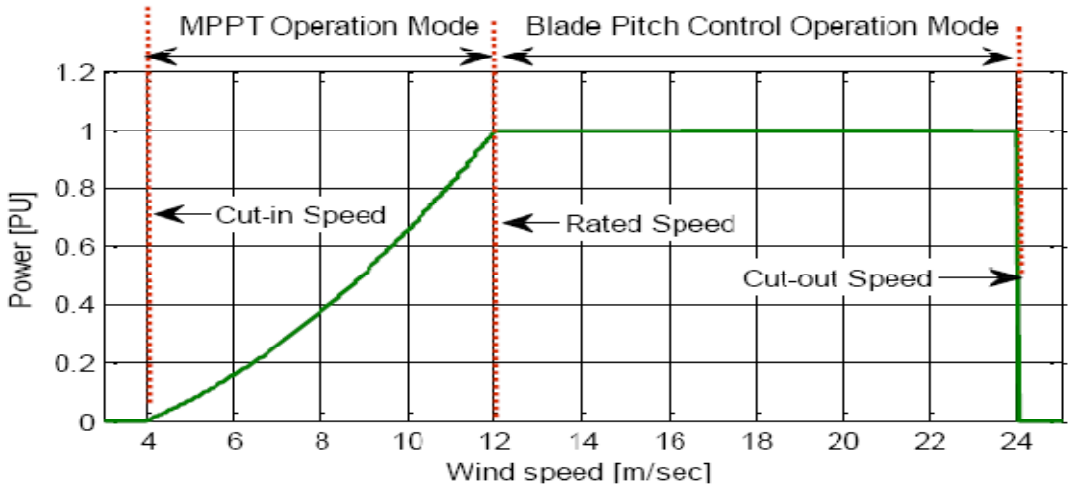

Figure 2.6 Power curve of a variable speed wind turbine

- Cut-in wind speed: The lowest wind speed at which wind turbine starts to generate power.
- Rated wind speed: Wind speed at which the wind turbine generates the rated power, which is usually the maximum power wind turbine can produce.
- Cut-out wind speed: Wind speed at which the turbine ceases power generation and is shut down (with automatic brakes and/or blade pitching) to protect the turbine from mechanical damage. [8]

2.4.4 TURBINE CLASSIFICATION AND ASSOCIATED GENERATOR SYSTEM

Based on the rotor-generator systems, turbines are classified into four types:[9]

Type A: Fixed speed.

Type B: Limited variable speed.

Type C: Variable speed with partial scale energy converter.

Type D: Variable speed with full scale energy converter.

Type A: Fixed Speed

- SCIG (Squirrel cage induction generator) directly connected to the grid via a transformer.

- SCIG draws reactive power from the grid that is compensated by the capacitor bank (in the absence of the capacitor bank voltage fluctuations and power line losses inevitable)
- Wind speed variability imposes high stresses on the turbine structure.

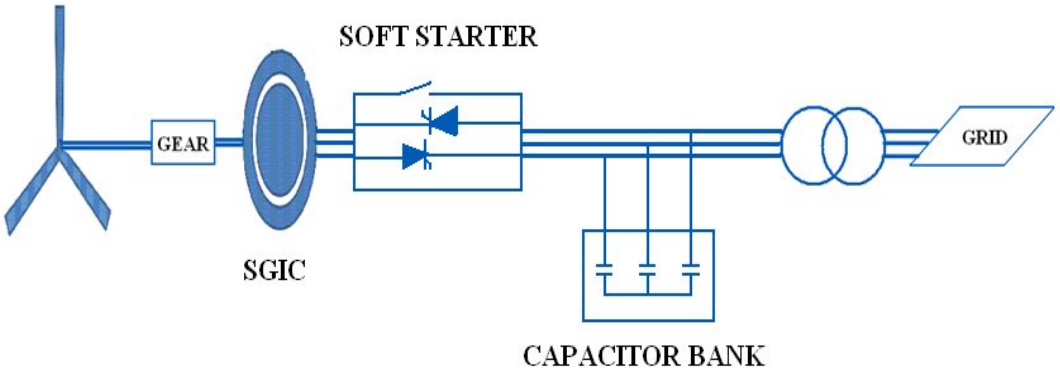

Figure 2.7 Type A: Fixed Speed

Type B: Limited Variable Speed

- WRIG (Wound rotor induction generator) directly connected to the grid and it uses a capacitor bank.
- Soft-starter ensures smother grid connection.
- The rotor resistance is controllable and thus the power output is controlled.
- The rotor resistance is changed by an optically controlled converter mounted on the rotor shaft (the OptiSlip concept)
- The rotor controllable speed range is 0% to 10% over the synchronous speed and it is rotor size dependent.

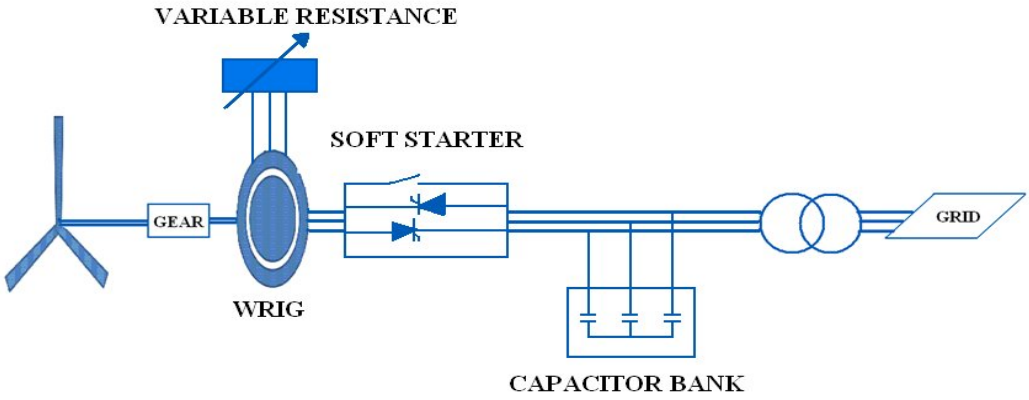

Figure 2.8 Type B: Limited Variable Speed

Type C: Variable Speed with Partial Scale Energy Converter

- The configuration known as DFIG (Double fed induction generator) correspond to the WRIG (Wound rotor induction generator) with partial scale frequency converter.
- The partial scale frequency converter performs the reactive power compensation and ensures smoother grid connection.
- Partial Scale Energy Converter power compensation and ensures smoother grid connection.
- The generator has a wider range of speed control, e.g., (-40% to +30%) around the synchronous speed (wider than OptiSlip)
- The use of slip rings and protection in case of grid faults is a major drawback.

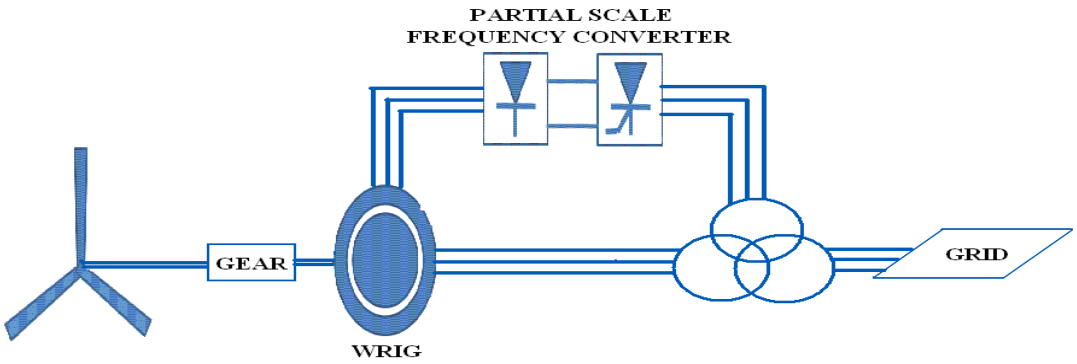

Figure 2.9 Type C: Variable Speed with Partial Scale Energy Converter.

Type D: Variable Speed with Full Scale Energy Converter

In this configuration we may use:

- PMSG (Permanent magnet squirrel generator) or
- WRSG (Wound rotor synchronous generator) or
- WRIG (Wound rotor induction generator)
- The full-scale frequency converter performs the reactive power compensation and ensures smoother grid connection.
- May not use a gearbox at all.
- Turbine examples: Enercon, Made, and Lagerwey.

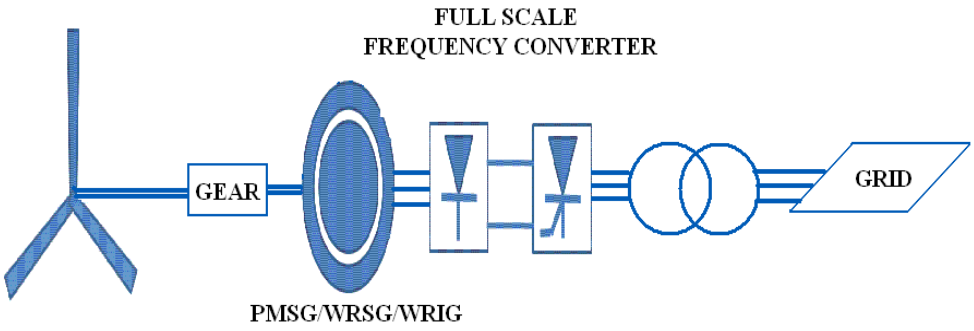

Figure 2.10 Type D: Variable Speed with Full Scale Energy Converter

2.5 MODELING OF WIND TURBINE

From the physical point of view, the static characteristics of wind turbine rotor can be defined by relationship between the total power in wind and the mechanical power of wind turbine. These relationships are readily described starting with the incoming wind in the rotor swept area. It can be shown that the kinetic energy of a cylinder of air of radius R travelling at wind speed V_{wind} corresponding to a total wind power P_{wind} within the rotor swept of the wind turbine. The P_{wind} can be expressed as, [9]

$$P_{wind} = 0.5\rho_{air}\pi R^2 V^3{}_{wind} \tag{2.1}$$

Where, ρ_{air} is the air density (1.225 kg/m^3)

R is the radius

And V_{wind} is the wind speed.

It is possible to extract all the kinetic energy from the wind since this would mean that the air would stand still directly behind the wind turbine. This would not allow the air to flow away from the wind turbine, and clearly this cannot represent a physical steady-state condition. The wind speed is only reduced by the wind turbine, which thus extracts a fraction of the power of wind. This fraction is expressed as the power efficient coefficient, C_p, of wind turbine. Therefore the mechanical power output of the wind turbine P_{mech} considering the definition of C_p can be stated as given by

$$P_{mech} = C_p P_{wind} \tag{2.2}$$

Therefore, equation (2.1) can be written as,

$$P_{mech} = 0.5 C_p \rho_{air} \pi R^2 V^3_{wind} \tag{2.3}$$

It can be shown that the theoretical static upper limit of Cp is approximately 0.59, this suggests that 59% of the maximum kinetic energy can be extracted from the wind. This is known as Bets limit. Betz law says that we can only convert less than 16/27 (or 59.3%) of the kinetic energy in the wind to mechanical energy using a wind turbine. It is because the wind after passing through wind turbine still has some velocity. Within the turbine, most of the energy is converted into useful electrical energy, while some of it is lost in gearbox, bearings, generator, power converter, transmission and others. Most practical rotors with three blades can reach an overall efficiency of about 50%.

From physical point of view the power, P_{mech} that is extracted from the wind will depend on rotational speed, wind speed and the blade angle, β. Therefore, P_{mech} and Cp are functions of these parameters.

$$P_{mech} = f(\omega_{turb}, V_{wind}, \beta) \tag{2.4}$$

The forces of the wind on a blade section and thereby the possible energy extraction will depend on the angle of incidence Ψ between the plane of the moving rotor blades and the relative wind speed V_{rel} as seen from the moving blades. Simple geometric consideration is shown in figure 2.5 the wind turbulence created by the blade tips has been ignored and the angle if incidence Ψ is determined by the incoming wind speed V_{wind} and the speed of the blade.

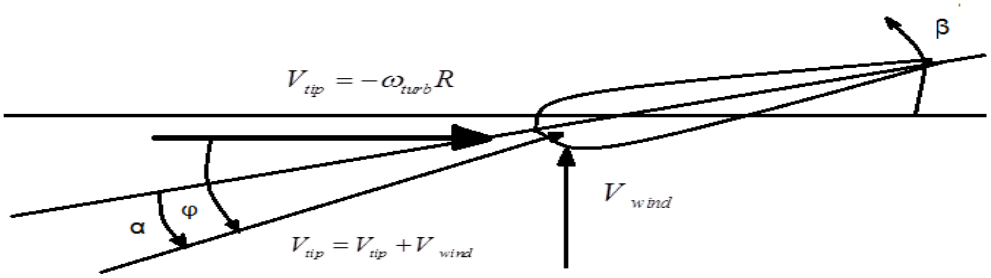

Figure 2.11 Illustration of forces around the moving blade

The blade tip is moving at wind speed V_{wind}, equal to (ω_{turb}*R). The highest values of Cp are typically obtained in range 8 to 9 (i.e when the tip of the blade moves 8 to 9 times faster than

the incoming wing). This means the angle between the relative air speed from the blade tip and rotor plane is rather a sharp angle.

Where V_{tip} = tip speed; ω_{turb}= turbine speed; R= rotor radius; V_{rel}= relative wind speed; V_{wind} = wind speed; α = angle of attack; Ψ = angle of incidence between the plane of the rotor and V_{rel}; β = blade angle.

On modern wind turbines it is possible to adjust the pitch angle β of the entire blade through servo mechanism. If the blade is turned, the angle of attack α between the blade and the relative wind V_{rel} will be changed accordingly. Again, it is clear from a physical perspective that the force of the relative and on the blade, and thereby the energy extraction, will depend on the angle of attack α between the moving rotor blades and the relative wind speed V_{rel} as seen from the moving blades. Hence C_p can be expresses as a function of λ and β.

$$C_p = f(\lambda, \beta) \tag{2.5}$$

CHAPTER-3

INTRODUCTION TO DFIG AND STEADY STATE ANALYSIS OF DFIG

3.1 GENERAL

With increased penetration of wind power into electrical grids, DFIG wind turbines are largely deployed due to their variable speed feature and hence influencing system dynamics. This has created an interest in developing suitable models for DFIG to be integrated into power system studies. The continuous trend of having high penetration of wind power, in recent years, has made it necessary to introduce new practices. For example, grid codes are being revised to ensure that wind turbines would contribute to the control of voltage and frequency and also to stay connected to the host network following a disturbance.

This chapter introduces the operation and control of a Doubly-fed Induction Generator (DFIG) system. The DFIG is currently the system of choice for multi-MW wind turbines. The aerodynamic system must be capable of operating over a wide wind speed range in order to achieve optimum aerodynamic efficiency by tracking the optimum tip-speed ratio. Therefore, the generator's rotor must be able to operate at a variable rotational speed. The DFIG system therefore operates in both sub- and super-synchronous modes with a rotor speed range around the synchronous speed. The stator circuit is directly connected to the grid while the rotor winding is connected via slip-rings to a three-phase converter. For variable-speed systems where the speed range requirements are small, for example ±30% of synchronous speed, the DFIG offers adequate performance and is sufficient for the speed range required to exploit typical wind resources.

An AC-DC-AC converter is included in the induction generator rotor circuit. The power electronic converters need only be rated to handle a fraction of the total power – the rotor power – typically about 30% nominal generator power. Therefore, the losses in the power electronic converter can be reduced, compared to a system where the converter has to handle the entire power, and the system cost is lower due to the partially-rated power electronics. This chapter will introduce the basic features and normal operation of DFIG systems for wind power applications basing the description on the standard induction

generator. Different aspects that will be described include their variable-speed feature, power converters and their associated control systems, and application issues.

3.2 DOUBLY FED INDUCTION GENERATOR

Wind turbines use a doubly-fed induction generator (DFIG) consisting of a wound rotor induction generator and an AC/DC/AC IGBT- converter. The stator winding is connected directly to the 50 Hz grid while the rotor is fed at variable frequency through the AC/DC/AC converter. The DFIG technology allows extracting maximum energy from the wind for low wind speeds by optimizing the turbine speed, while minimizing mechanical stresses on the turbine during gusts of wind. The optimum turbine speed producing maximum mechanical energy for a given wind speed is proportional to the wind speed. Another advantage of the DFIG technology is the ability for power electronic converters to generate or absorb reactive power, thus eliminating the need for installing capacitor banks as in the case of squirrel-cage induction generator.[15]

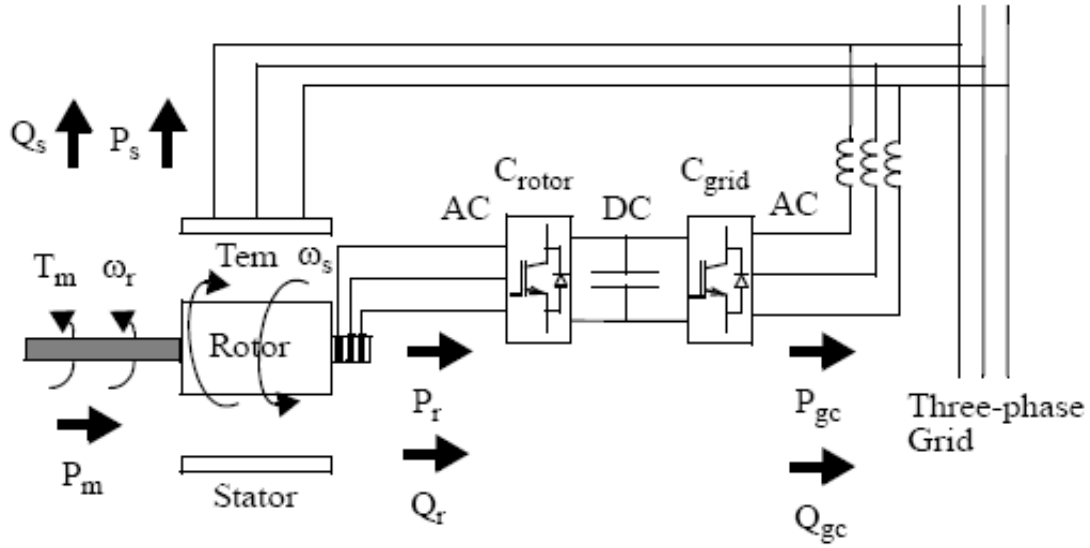

Figure 3.1 Basic diagram of doubly fed induction generator with converter

Where V_r is the rotor voltage and V_{gc} is grid side voltage. The AC/DC/AC converter is basically a PWM converter which uses sinusoidal PWM technique to reduce the harmonics present in the wind turbine driven DFIG system. Here C_{rotor} is rotor side converter and C_{grid} is grid side converter. To control the speed of wind turbine gear boxes or electronic control can be used.

3.2.1 OPERATING PRINCIPLE OF DFIG

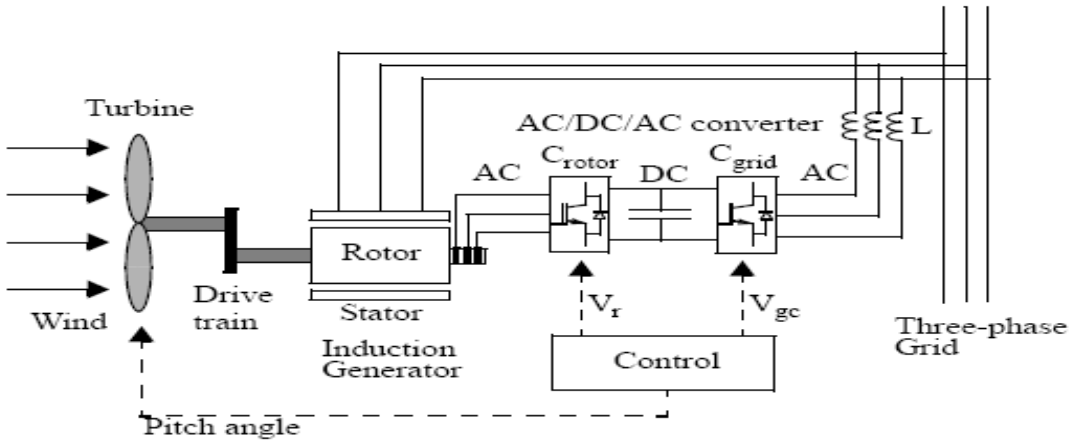

Figure 3.2 Power flow diagram of DFIG

The stator is directly connected to the AC mains, while the wound rotor is fed from the Power Electronics Converter via slip rings to allow DIFG to operate at a variety of speeds in response to changing wind speed. Indeed, the basic concept is to interpose a frequency converter between the variable frequency induction generator and fixed frequency grid. The DC capacitor linking stator- and rotor-side converters allows the storage of power from induction generator for further generation. To achieve full control of grid current, the DC-link voltage must be boosted to a level higher than the amplitude of grid line-to-line voltage. The slip power can flow in both directions, i.e. to the rotor from the supply and from supply to the rotor and hence the speed of the machine can be controlled from either rotor- or stator-side converter in both super and sub-synchronous speed ranges.[18-23]

As a result, the machine can be controlled as a generator or a motor in both super and sub-synchronous operating modes realizing four operating modes. Below the synchronous speed in the motoring mode and above the synchronous speed in the generating mode, rotor-side converter operates as a rectifier and stator-side converter as an inverter, where slip power is returned to the stator. Below the synchronous speed in the generating mode and above the synchronous speed in the motoring mode, rotor-side converter operates as an inverter and stator side converter as a rectifier, where slip power is supplied to the rotor. At the synchronous speed, slip power is taken from supply to excite the rotor windings and in this case machine behaves as a synchronous machine.

The mechanical power and the stator electric power output are computed as follows:

$$P_r = T_m \times \omega_r \tag{3.1}$$

$$P_s = T_{em} \times \omega_s \tag{3.2}$$

For a loss less generator the mechanical equation is:

$$J \frac{d\omega_r}{dt} = T_m + T_{em} \tag{3.3}$$

In steady-state at fixed speed for a loss less generator

$$T_m = T_{em} \tag{3.4}$$

And

$$P_m = P_s + P_r \tag{3.5}$$

and It follows that:

$$P_r = P_m - P_s = T_m \omega_r - T_{em} \omega_s = -sP_s \tag{3.6}$$

Where,

$s = (\omega_s - \omega_r)/\omega_s$ is defined as the slip of the generator. Generally the absolute value of slip is much lower than 1 and, consequently, P_r is only a fraction of P_s. Since T_m is positive for power generation and since ω_s is positive and constant for a constant frequency grid voltage, the sign of P_r is a function of the slip sign. P_r is positive for negative slip (speed greater than synchronous speed) and it is negative for positive slip (speed lower than synchronous speed). For super-synchronous speed operation, P_r is transmitted to DC bus capacitor and tends to raise the DC voltage.[14]

For sub-synchronous speed operation, Pr is taken out of DC bus capacitor and tends to decrease the DC voltage. C_{grid} is used to generate or absorb the power P_{gc} in order to keep the DC voltage constant. In steady-state for a lossless AC/DC/AC converter P_{gc} is equal to Pr and the speed of the wind turbine is determined by the power Pr absorbed or generated by C_{rotor}. The phase-sequence of the AC voltage generated by C_{rotor} is positive for sub-synchronous speed and negative for super synchronous speed. The frequency of this voltage is equal to the product of the grid frequency and the absolute value of the slip. C_{rotor} and C_{grid} have the capability for generating or absorbing power and could be used to control the power or the voltage at the grid terminals.

3.2.2 ROTOR SIDE CONVERTER CONTROL SYSTEM

The rotor-side converter is used to control the wind turbine output power and the voltage (or reactive power) measured at the grid terminals. The power is controlled in order to follow a pre-defined power-speed characteristic, named tracking characteristic. An example of such a characteristic is illustrated in the figure called Turbine Characteristics and Tracking Characteristic, by the ABCD curve superimposed to the mechanical power characteristics of the turbine obtained at different wind speeds. The actual speed of the turbine ω_r is measured and the corresponding mechanical power of the tracking characteristic is used as the reference power for the power control loop. The tracking characteristic is defined by four points: A, B, C and D. From zero speed to speed of point A the reference power is zero. Between point A and point B the tracking characteristic is a straight line, the speed of point B must be greater than the speed of point A. [13] Between point B and point C the tracking characteristic is the locus of the maximum power of the turbine (maxima of the turbine power Vs turbine speed curves). The tracking characteristic is a straight line from point C and point D. The power at point D is one per unit (1 pu) and the speed of the point D must be greater than the speed of point C. Beyond point D the reference power is a constant equal to one per unit (1 pu).[20]

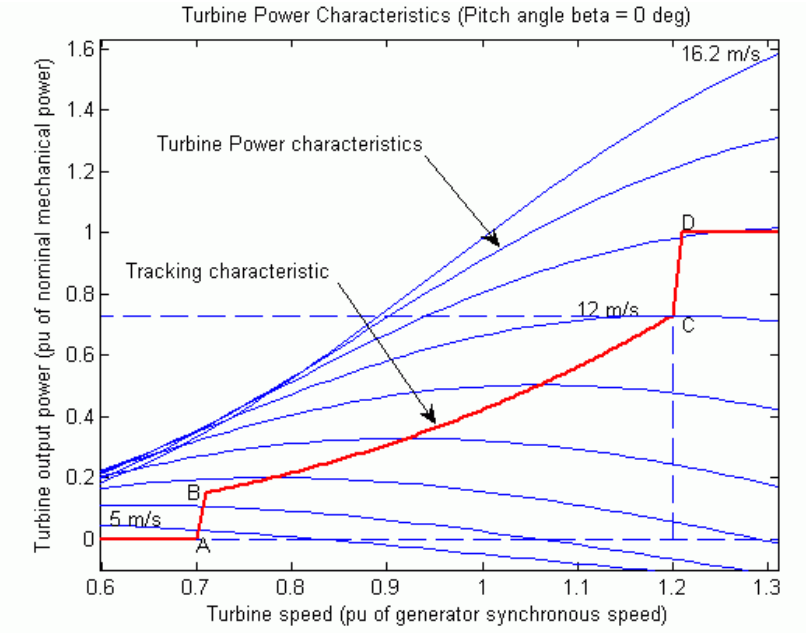

Figure 3.3 Turbine Characteristics and Tracking Characteristic [20]

The actual electrical output power, measured at the grid terminals of the wind turbine, is added to the total power losses (mechanical and electrical) and is compared with the

reference power obtained from the tracking characteristic. A Proportional-Integral (PI) regulator is used to reduce the power error to zero. The output of this regulator is the reference rotor current I_{qr}_ref that must be injected in the rotor by converter C_{rotor}. This is the current component that produces the electromagnetic torque T_{em}. The actual I_{qr} component of positive-sequence current is compared to I_{qr}_ref and the error is reduced to zero by a current regulator (PI). The output of this current controller is the voltage V_{qr} generated by C_{rotor}. The current regulator is assisted by feed forward terms which predict V_{qr}.[20]

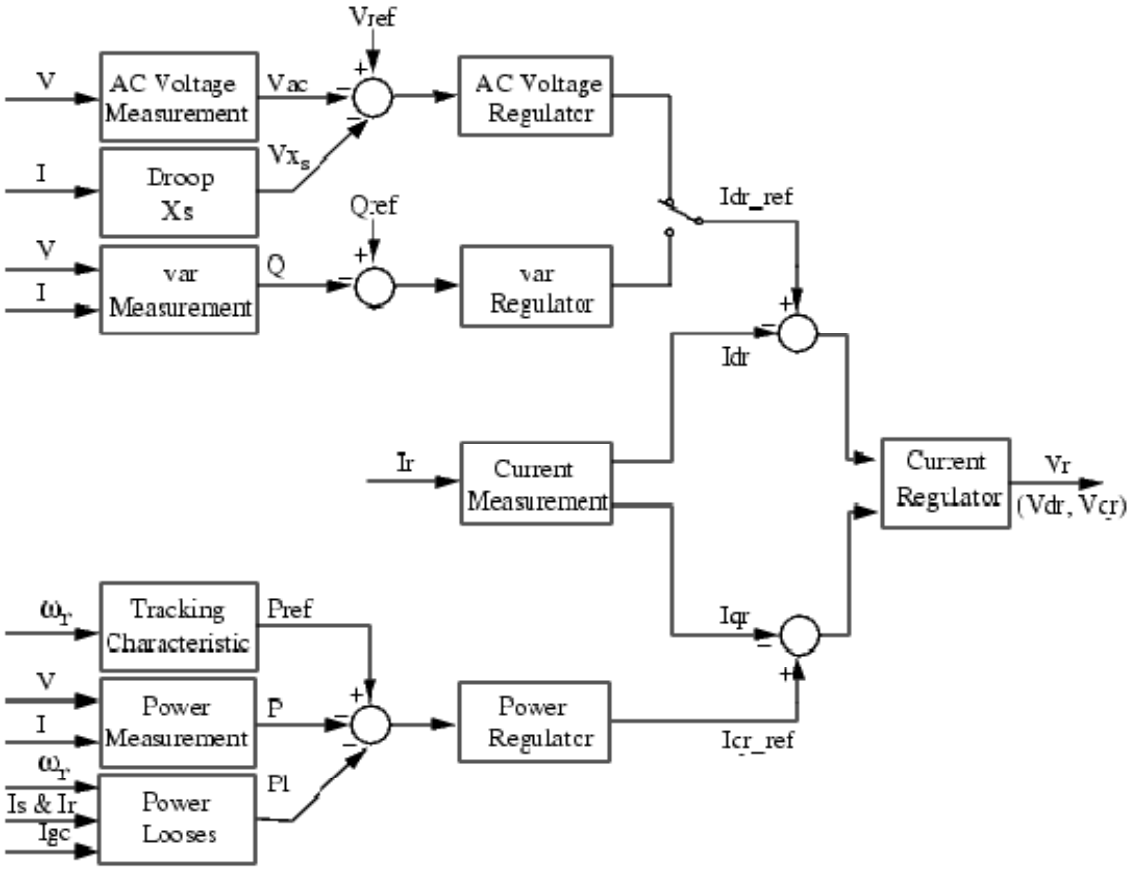

Figure 3.4 Rotor-Side Converter Control System

The voltage or the reactive power at grid terminals is controlled by the reactive current flowing in the converter C_{rotor}. The generic control loop is illustrated in the figure called Rotor-Side Converter Control System.[21-23]

When the wind turbine is operated in voltage regulation mode, it implements the following V-I characteristic.

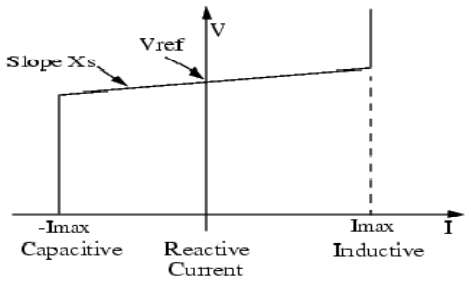

Fig. 3.5 Turbine V-I Characteristic

As long as the reactive current stays within the maximum current values (-Imax, Imax) imposed by the converter rating, the voltage is regulated at the reference voltage V_{ref}. However, a voltage droop is normally used (usually between 1% and 4% at maximum reactive power output), and the V-I characteristic has the slope indicated in the figure called Wind Turbine V-I Characteristic. In the voltage regulation mode, the V-I characteristic is described by the following equation:[14]

$$V = V_{\text{ref}} + X_s I$$

Where,

V	Positive sequence voltage (pu)
I	Reactive current (pu/P_{nom}) (I > 0 indicates an inductive current)
X_s	Slope or droop reactance (pu/P_{nom})
P_{nom}	Three-phase nominal power of the converter specified in the block dialog box

When the wind turbine is operated in var regulation mode the reactive power at grid terminals is kept constant by a var regulator.

The output of the voltage regulator or the var regulator is the reference d-axis current I_{dr}_ref that must be injected in the rotor by converter C_{rotor}. The same current regulator as for the power control is used to regulate the actual I_{dr} component of positive-sequence current to its reference value. The output of this regulator is the d-axis voltage V_{dr} generated by C_{rotor}. The current regulator is assisted by feed forward terms which predict V_{dr}.

V_{dr} and V_{qr} are respectively the d-axis and q-axis of the voltage V_r.

Note:

- For C_{rotor} control system and measurements the d-axis of the d-q rotating reference frame is locked on the generator mutual flux by a PLL which is assumed to be ideal in this phasor model.
- The magnitude of the reference rotor current I_r_ref is equal to $\sqrt{I_{dr\_ref}^2 + I_{qr\_ref}^2}$ The maximum value of this current is limited to 1 pu. When I_{dr}_ref and I_{qr}_ref are such that the magnitude is higher than 1 pu the I_{qr}_ref component is reduced in order to bring back the magnitude to 1 pu.

3.2.3 GRID SIDE CONTROL SYSTEM

The converter C_{grid} is used to regulate the voltage of the DC bus capacitor. In addition, this model allows using C_{grid} converter to generate or absorb reactive power.The control system, illustrated in the fig. 3.6 called Grid-Side Converter Control System, consists of:

- Measurement systems measuring the d and q components of AC positive-sequence currents to be controlled as well as the DC voltage V_{dc}.
- An outer regulation loop consisting of a DC voltage regulator. The output of the DC voltage regulator is the reference current I_{dgc}_ref for the current regulator (I_{dgc}= current in phase with grid voltage which controls active power flow).[17]
- An inner current regulation loop consisting of a current regulator. The current regulator controls the magnitude and phase of the voltage generated by converter C_{grid} (V_{gc}) from the I_{dgc}_ref produced by the DC voltage regulator and specified I_q_ref reference. The current regulator is assisted by feed forward terms which predict the C_{grid} output voltage.

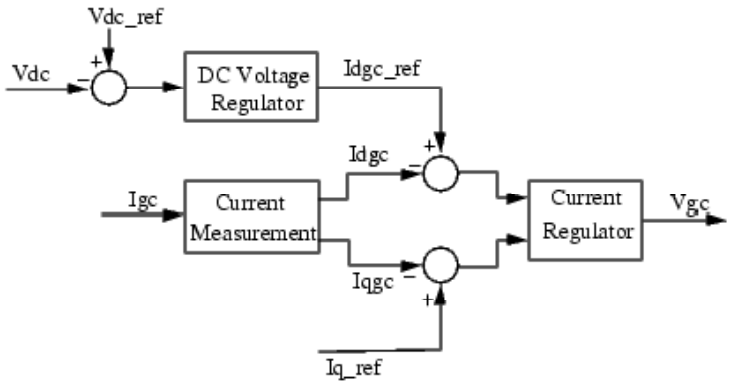

Figure 3.6 Grid-Side Converter Control System

- The magnitude of the reference grid converter current I_{gc}_ref is equal to $\sqrt{I^2_{d\_gc\_ref} + I^2_{q\_ref}}$ The maximum value of this current is limited to a value defined by the converter maximum power at nominal voltage. When I_{dgc}_ref and I_d_ref are such that the magnitude is higher than this maximum value the I_q_ref component is reduced in order to bring back the magnitude to its maximum value.[20]

3.2.4 PITCH ANGLE CONTROL SYSTEM

The pitch angle is kept constant at zero degree until the speed reaches point D speed of the tracking characteristic. Beyond point D the pitch angle is proportional to the speed deviation from point D speed. The control system is illustrated in the following figure 3.7[16]

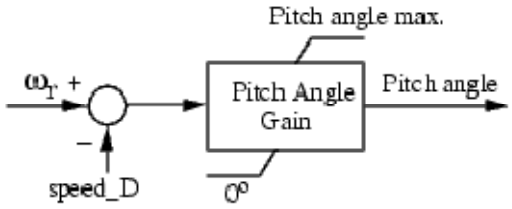

Figure 3.7 Pitch Control System

3.3 INTRODUCTION TO LOAD FLOW

In a three phase ac power system active and reactive power flows from the generating station to the load through different networks buses and branches. The flow of active and reactive power is called power flow or load flow. Power flow studies provide a systematic mathematical approach for determination of various bus voltages, there phase angle active and reactive power flows through different branches, generators and loads under steady state condition. Power flow analysis is used to determine the steady state operating condition of a power system. Power flow analysis is widely used by power distribution professional during the planning and operation of power distribution system.

3.4 OBJECTIVE OF LOAD FLOW STUDY

- Power flow analysis is very important in planning stages of new networks or addition to existing ones like adding new generator sites, meeting increase load demand and locating new transmission sites.

- The load flow solution gives the nodal voltages and phase angles and hence the power injection at all the buses and power flows through interconnecting power channels.
- It is helpful in determining the best location as well as optimal capacity of proposed generating station, substation and new lines.
- It determines the voltage of the buses. The voltage level at the certain buses must be kept within the closed tolerances.
- System transmission loss minimizes.
- Economic system operation with respect to fuel cost to generate all the power needed
- The line flows can be known. The line should not be overloaded, it means, we should not operate the close to their stability or thermal limits.

3.5 BUS CLASSIFICATION

A bus is a node at which one or many lines, one or many loads and generators are connected. In a power system each node or bus is associated with 4 quantities, such as magnitude of voltage, phage angle of voltage, active or true power and reactive power in load flow problem two out of these 4 quantities are specified and remaining 2 are required to be determined through the solution of equation. Depending on the quantities that have been specified, the buses are classified into 3 categories.

Buses are classified according to which two out of the four variables are specified as:

1. **Load bus**: No generator is connected to the bus. At this bus the real and reactive power are specified. It is desired to find out the voltage magnitude and phase angle through load flow solutions. It is required to specify only Pd and Qd at such bus as at a load bus voltage can be allowed to vary within the permissible values.

2. **Generator bus or voltage controlled bus**: Here the voltage magnitude corresponding to the generator voltage and real power Pg corresponds to its rating are specified. It is required to find out the reactive power generation Qg and phase angle of the bus voltage.

3. **Slack (swing) bus**: For the Slack Bus, it is assumed that the voltage magnitude $|V|$ and voltage phase θ are known, whereas real and reactive powers Pg and Qg are obtained through the load flow solution.

3.6 FORMULATION OF THE LOAD FLOW PROBLEM

Load flow studies are based on a nodal voltage analysis of a power system. As an example, consider the very simple system represented by the single-line diagram in Fig. 3.8. Here two generators (1 and 2) are interconnected by one transmission line and are separately connected to a load (3) by two other lines. If the phasor currents injected into the system are I_1, I_2, and I_3, and the lines are modelled by simple series admittances, then it is possible to draw the equivalent circuit for one representative phase of the balanced three-phase system, as shown in Fig. 3.12.

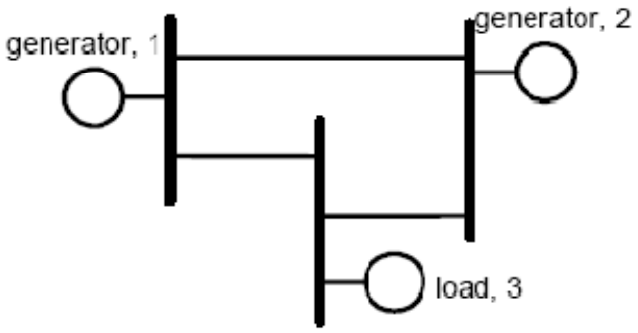

Fig. 3.8 Single-line diagram of a simple example power system.

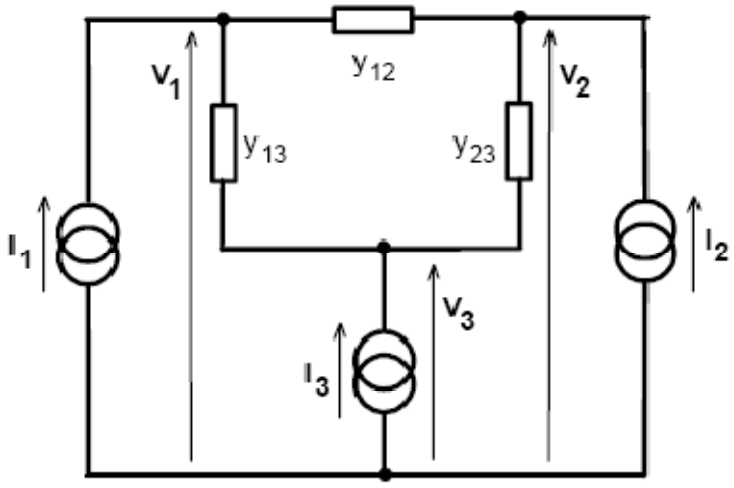

Fig. 3.9 Equivalent circuit for one phase of the system shown in Fig.3.8

For the circuit in Figure 3.9 the nodal voltage equations can be written directly. For example, at node 1:

$$I_1 = (Y_{12} + Y_{13})V_1 - Y_{12}V_2 - Y_{13}V_3 \qquad (3.33)$$

In general, for a system with r nodes, then at node n:

$$I_n = Y_{n1}V_1 + Y_{n2}V_2 + ... + Y_{nn}V_n + ... + Y_{nr}V_r = \sum_{k=1}^{r} Y_{nk}V_k \qquad (3.34)$$

Where, Y_{nn} = sum of all admittances connected to node n

Y_{nk} = - (sum of all admittances connected between nodes n and k)

I_n = current injected at node n

For the complete system of r nodes:

$$\begin{bmatrix} I_1 \\ . \\ . \\ I_n \\ . \\ . \\ I_r \end{bmatrix} = \begin{bmatrix} Y_{11} & . & . & Y_{1n} & . & . & Y_{1r} \\ . & & & . & & & . \\ . & & & . & & & . \\ Y_{n1} & . & . & Y_{nn} & . & . & Y_{nr} \\ . & & & . & & & . \\ . & & & . & & & . \\ Y_{r1} & . & . & Y_{rn} & . & . & Y_{rr} \end{bmatrix} \cdot \begin{bmatrix} V_1 \\ . \\ . \\ V_n \\ . \\ . \\ V_r \end{bmatrix} \text{ or } [I] = [Y].[V] \qquad (3.35)$$

Where, [Y] is the nodal admittance matrix. Formulation of the load flow problem is most conveniently carried out with the terms in the nodal admittance matrix expressed in polar notation: $Y_{kn} = |Y_{kn}| \angle \theta_{kn}$. The Excel Workbook (Sheet 2) allows users to enter series impedance data for the three lines and then automatically calculates the terms in the nodal admittance matrix.

Conventional circuit analysis proceeds directly from equation (3.35) by inverting the nodal admittance matrix and hence solving for the nodal voltages [V]. However, the load flow problem is complicated by the lack of uniformity in the data about electrical conditions at the nodes. There are three distinct types of nodal data, which relate to the physical nature of the power system:

a) Load nodes, where complex power $S_{ns} = P_{ns} + jQ_{ns}$ taken from or injected into the system is defined. Such nodes may also include links to other systems. At these load nodes, the voltage magnitude |Vn| and phase angle δn must be calculated.

b) Generator nodes, where the injected power, P_{ns}, and the magnitude of the nodal voltage |Vn| are specified. These constraints reflect the generator's operating characteristics, in which power is controlled by the governor and terminal voltage is controlled by the automatic voltage regulator. At the generator nodes the voltage phase angle δ_n must be calculated.

c) At least one node, termed the 'floating bus' or 'slack bus', where the nodal voltage magnitude |Vn| and phase angle δ_n are specified. This node acts as the reference node and is commonly chosen to have a phase angle $\delta_n = 0^o$. The power and reactive power delivered at this node are not specified.

In the system configuration of Figure 3.11, which is analyzed in the Excel Workbook, each type of node is represented with node 1 being a floating bus, node 2 being a generator node and node 3 being a load node. Consequently values must be specified for the power (P_{2s}) injected at node 2, and the power (P_{3s}) and reactive power (Q_{3s}) injected at node 3. All three of these power values may be changed by the user, though default values are provided (P_{2s} = 1.0; P_{3s} = -1.5; Q_{3s} = -0.2), with negative values indicating that power or reactive power is being drawn from the system. The magnitude of the voltage at node 1 can be specified, with the default value being 1.0 pu, while the phase angle is fixed at 0^o ($V_2 = 1.0\angle 0$). At the generator node (node 2), the voltage magnitude can be set by the user with the default value being 1.1 pu ($V_2 = 1.1\angle\delta_2$), and the phase angle δ_2 is calculated during the load flow solution. At the load node (node 3) the voltage magnitude and phase angle have to be calculated ($V_3 = |V_3|\angle\delta_2$). So the complete load flow problem for this particular power system configuration involves the calculation of the voltage magnitude $|V_3|$ V_3 and the phase angles δ_2, δ_3.

3.7 NEWTON RAPHSON METHOD

General Approach

The Newton-Raphson method is an iterative technique for solving systems of simultaneous equations in the general form:

$$f_1(X_1 \ldots X_n \ldots X_r) = K_1$$
$$f_j(X_1 \ldots X_n \ldots X_r) = K_n \qquad (3.36)$$
$$f_n(X_1 \ldots X_n \ldots X_r) = K_r$$

where f_1,.... f_n.... f_r are differentiable functions of the variables X_1,.... X_n ,.... X_r and K_1, ... K_n.... K_r are constants. Applied to the load flow problem, the variables are the nodal voltage magnitudes and phase angles, the functions are the relationships between power, reactive power and node voltages, while the constants are the specified values of power and reactive power at the generator and load nodes.

Power and reactive power functions can be derived by starting from the general expression for injected current (Eqn. 3.34) at node n:

$$I_n = \sum_{k=1}^{r} Y_{nk} V_k$$

so the complex power input to the system at node n is:

$$S_n = V_n I_n^* \tag{3.37}$$

Where the superscript * denotes the complex conjugate. Substituting from (3.34) with all complex variables written in polar form:

$$S_n = V_n \sum_{k=1}^{r} Y_{nk}^* V_k^* = \sum_{k=1}^{r} |V_n||V_k||Y_{nk}| \angle \{\delta_n - \delta_k - \theta_{nk}\} \tag{3.38}$$

The power and reactive power inputs at node n are derived by taking the real and imaginary parts of the complex power:

$$P_n = \{S_n\} = \sum_{k=1}^{r} |V_n||V_k||Y_{nk}| \cos\{\delta_n - \delta_k - \theta_{nk}\} \tag{3.39}$$

$$Q_n = \{S_n\} = \sum_{k=1}^{r} |V_n||V_k||Y_{nk}| \sin\{\delta_n - \delta_k - \theta_{nk}\} \tag{3.40}$$

The load flow problem is to find values of voltage magnitude and phase angle, which, when substituted into (3.39) and (3.40), produce values of power and reactive power equal to the specified set values at that node, P_{ns} and Q_{ns}.

The first step in the solution is to make initial estimates of all the variables: $|V_n^o|, \delta_n^0$ where the superscript ^{0} indicates the number of iterative cycles completed. Using these estimates, the power and reactive power input at each node can be calculated from (3.39) and (3.40). These values are compared with the specified values to give a power and reactive power error. For node n:

$$P_n^0 = P_{ns} - \sum_{k=1}^{r} |V_n^0||V_k^0||Y_{nk}| \cos\{\delta_n^0 - \delta_k^0 - \theta_{nk}\} \tag{3.41}$$

$$Q_n^0 = Q_{ns} - \sum_{k=1}^{r} |V_n^0||V_k^0||Y_{nk}| \sin\{\delta_n^0 - \delta_k^0 - \theta_{nk}\} \tag{3.42}$$

The power and reactive power errors at each node are related to the errors in the voltage magnitudes and phase angles, e.g. $\Delta|V_n|^o$, $\Delta\delta_n^0$, by the first order approximations:

$$\begin{bmatrix} \vdots \\ \Delta P_n^0 \\ \vdots \\ \Delta Q_n^0 \\ \vdots \end{bmatrix} = \begin{bmatrix} \cdots & \cdots & \cdots & \cdots & \cdots & \cdots & \cdots & \cdots & \cdots \\ \frac{\partial P_n}{\partial \delta_{n-1}} & \frac{\partial P_n}{\partial \delta_n} & \frac{\partial P_n}{\partial \delta_{n+1}} & \cdots & \frac{\partial P_n}{\partial |V_{n-1}|} & \frac{\partial P_n}{\partial |V_n|} & \frac{\partial P_n}{\partial |V_{n+1}|} & \cdots \\ \cdots & \cdots & \cdots & \cdots & \cdots & \cdots & \cdots & \cdots \\ \frac{\partial Q_n}{\partial \delta_{n-1}} & \frac{\partial Q_n}{\partial \delta_n} & \frac{\partial Q_n}{\partial \delta_{n+1}} & \cdots & \frac{\partial Q_n}{\partial |V_{n-1}|} & \frac{\partial Q_n}{\partial |V_n|} & \frac{\partial Q_n}{\partial |V_{n+1}|} & \cdots \\ \cdots & \cdots & \cdots & \cdots & \cdots & \cdots & \cdots & \cdots \end{bmatrix} \begin{bmatrix} \Delta\delta_{n-1}^0 \\ \Delta\delta_n^0 \\ \Delta\delta_{n+1}^0 \\ \Delta|V_{n-1}|^0 \\ \Delta|V_n|^0 \\ \Delta|V_{n+1}|^0 \end{bmatrix} \tag{3.43}$$

Where the matrix of partial differentials is called the Jacobian matrix, [J]. The elements of the Jacobian are calculated by differentiating the power and reactive power expressions (3.39) and (3.40), and substituting the estimated values of voltage magnitude and phase angle.

At the next stage of the Newton-Raphson solution, the Jacobian is inverted. Matrix inversion is a computationally-complex task with the resources of time and storage increasing rapidly with the order of [J]. This requirement for matrix inversion is a major drawback of the Newton-Raphson method of load flow analysis for large-scale power systems. However, with the inversion completed, the approximate errors in voltage magnitudes and phase angles can be calculated by pre-multiplying both sides of (3.43):[25]

$$\begin{bmatrix} \Delta\delta_{n-1}^0 \\ \Delta\delta_n^0 \\ \Delta\delta_{n+1}^0 \\ \hline \Delta|V_{n-1}|^0 \\ \Delta|V_n|^0 \\ \Delta|V_{n+1}|^0 \end{bmatrix} = \left[J^0\right]^{-1} \begin{bmatrix} \vdots \\ \Delta P_n^0 \\ \vdots \\ \hline \vdots \\ \Delta Q_n^0 \\ \vdots \end{bmatrix} \tag{3.44}$$

The approximate errors from (3.44) are added to the initial estimates to produce new estimated values of node voltage magnitude and angle. For node n:

$$|V_n^1| = |V_n^0| + \Delta|V_n^0| \tag{3.45}$$

$$\delta_n^1 = \delta_n^0 + \Delta\delta_n^0 \tag{3.46}$$

Because first-order approximations are used in (3.43) the new estimates (denoted by the superscript 1) are not exact solutions to the problem. However, they can be used in another iterative cycle, involving the solution of Equations (3.41-3.46). The process is repeated until the differences between successive estimates are within an acceptable tolerance band.

The description above relates specifically to a load node, where there are two unknowns (the voltage magnitude and angle) and two equations relating to the specified power and reactive power. For a generator node the voltage magnitude *n V* and power *n P* are specified, but the reactive power is not specified. The order of the calculation can be reduced by 1. There is no need to ensure that the reactive power is at a set value and only the angle of the node voltage needs to be calculated, so one row and column are removed from the Jacobian. For the floating bus, both voltage magnitude and angle are specified, so there is no need to calculate these quantities. [9]

3.7.1 NEWTON-RAPHSON ALGORITHM

The Newton-Raphson procedure is as follows: [25]

Step-1: Read line data and bus data. The line data includes the line impedance and the transformer tap setting, the bus data include the type of bus load and generation level etc.

Step-2: Normalize the data to common base.

Step-3: Form the Y_{bus} using the line data.

Step-4: Set iter=0.

Step-5: Calculate the injected powers P_i and Q_i for all the buses except slack bus using eq. 3.41 and 3.42.

Step-6: Use the estimated V and δ to formulate the Jacobian matrix J.

Step-7: Solve eq. 3.44 to obtain the changes $\Delta\delta$ and $\left|\frac{\Delta V}{V}\right|$.

Step-8: Update the values of V and δ using eq. 3.47 and 3.48.

$$\delta = \delta + \Delta\delta \tag{3.47}$$

$$|V| = |V| + \left[1 + \frac{\Delta|V|}{|V|}\right] \tag{3.48}$$

Step-9: Check ΔP and ΔQ at all buses except slack bus. If ΔP and ΔQ within the tolerance then terminate the iterative process otherwise iter=iter+1 and go to step 5.The flow chart of the above algorithm has been illustrated in Figure 3.10.

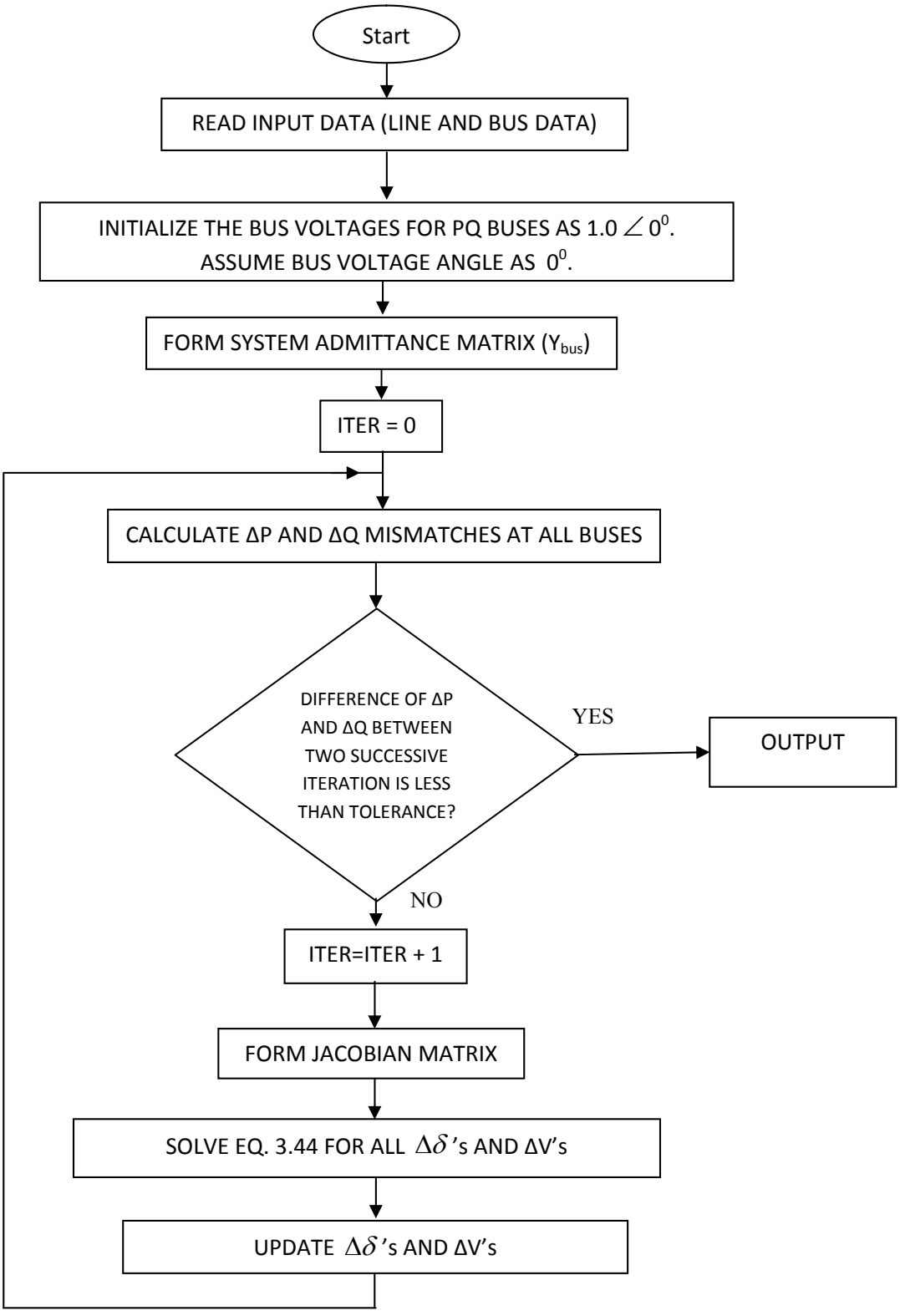

Figure 3.10 Flow chart for Newton-Raphson method

The basic information contained in the load-flow output is:

i) All bus voltage magnitudes and phase angles w.r.t the slack bus.

ii) All bus active and reactive power injections.

iii) All line sending- and receiving-end complex power flows.

iv) Individual line losses can be deduced by subtracting receiving-end complex power from sending-end complex power.

The most important information obtained from the load-flow is the voltage profile of the system. If $|V|$ varies greatly over the system, large reactive flows will result; this, in turn, will lead to increased real power losses and, in extreme cases, an increased likelihood of voltage collapse. When a particular bus has an unacceptably low voltage, the usual practice is to install capacitor banks in order to provide reactive compensation to the load. Load-flow studies are used to determine how much reactive compensation should be applied at a PQ bus, to bring its voltage up to an appropriate level.

3.8 STEADY STATE ANALYSIS OF DFIG

The typical configuration of a wind turbine based on a DFIG is shown in Figure 3.11. Its electrical single-phase equivalent circuits given in Figure.3.12. In the electrical circuit in Figure 3.12, the following expressions must be fulfilled:

$$V_s\angle\varphi_s = -\left(R_s + j\left(X_s + X_m\right)\right)I_s\angle\phi_s + jX_mI_r\angle\phi_r \tag{3.49}$$

$$V_r\angle\varphi_r = -jsX_mI_s\angle\phi_s + \left(R_r + js\left(X_s + X_m\right)\right)I_r\angle\phi_r \tag{3.50}$$

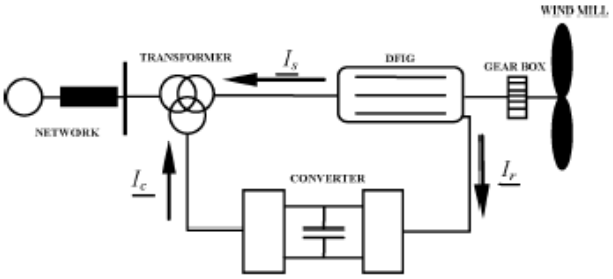

Figure 3.11 Configuration of a DFIG WT [24]

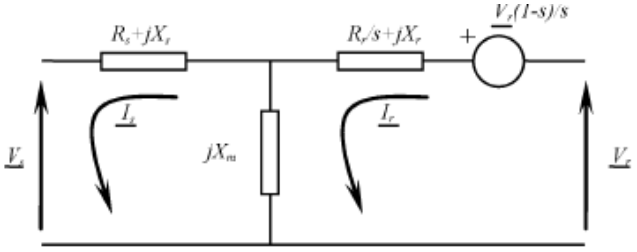

Figure 3.12 Equivalent electrical circuit of a DFIG [24]

This constitutes a set of two complex algebraic equations, that is, a set of four algebraic real equations, with eight unknown quantities, i.e., rms values and angles of rotor and stator voltages and currents. It will be shown that not all these variables are unknown, depending on the model chosen for the simulation.

Figure 3.12 shows a well-known model of the induction machine. In the case of the conventional machine the rotor voltage source equals 0 and the operating mode as generator or motor is given by the value of slip, s (s<0 gives a negative value of the total rotor resistor, and is assumed for generator mode). A very common approximation consists of neglecting the core losses.

They are generally modeled as a resistor with a value R_{Fe} in parallel with the magnetizing reactance X_m. From the point of view of calculation, taking into account these losses would only involve replacing the magnetizing impedance jX_m in (3.49) and (3.50) with an impedance obtained as the parallel of both impedances, i.e. $jR_{Fe}X_m /(R_{Fe}+X_m)$. In addition, (3.51) can be written according to the power balance, for obtaining, a power that will be called mechanical power, corresponding to the mechanical torque, or what is the same, the power the WT can extract from the wind, and that can be converted into the sum of rotor and stator active powers and losses:[24]

$$P_m = P_s + P_r + (I_s^2 R_s + I_r^2 R_r) = P + (I_s^2 R_s + I_r^2 R_r) \tag{3.51}$$

In terms of the electrical variables in (3.49) and (3.50), (3.51) can be alternatively written as in (3.52):

$$P_m = V_s I_s \cos(\varphi_s - \varphi_s) + V_r I_r \cos(\varphi_r - \varphi_r) + \left(I_s^2 R_s + I_r^2 R_r\right) \tag{3.52}$$

where a new unknown, P_m can appear depending on the model chosen for the bus, as will be described later. The reactive power exchanged between the machine and the network can be controlled up to certain limits. If the reactive power between the network side converter of the rotor and the network is fixed to 0, then all the reactive power exchange takes place through the stator. In this case, generated reactive power can be expressed as in (3.53):

$$Q_s = V_s I_s \sin(\varphi_s - \varphi_s) \tag{3.53}$$

As a summary, in order to use the NR technique for solving the set of nonlinear equations, the following functions are defined, and the goal is to force them to converge to 0:

$$f_1 = V_s \cos\varphi_s + R_s I_s \cos\phi_s - (X_s + X_m) I_s \sin\phi_s + X_m I_r \sin\phi_r \tag{3.54}$$

$$f_2 = V_s \sin\varphi_s + R_s I_s \sin\phi_s - (X_s + X_m) I_s \cos\phi_s + X_m I_r \cos\phi_r \tag{3.55}$$

$$f_3 = V_r \cos\varphi_r + R_r I_r \cos\phi_r + s(X_r + X_m) I_r \sin\phi_r + sX_m I_s \sin\phi_s \tag{3.56}$$

$$f_4 = V_r \sin\varphi_r + R_r I_r \sin\phi_r - s(X_r + X_m) I_r \sin\phi_r + sX_m I_s \cos\phi_s \tag{3.57}$$

$$f_5 = P - V_s I_s \cos(\varphi_s - \phi_s) + V_s I_s \cos(\varphi_r - \phi_r) \tag{3.58}$$

$$f_6 = Q - V_s I_s \sin(\varphi_s - \phi_s) \tag{3.59}$$

$$f_7 = P - k_0 (1-s)^3 + (I_s^2 R_s + I_r^2 R_r) \tag{3.60}$$

$$\Delta f = \Delta \left(f_1 f_2 ... f_7 \right)^T \tag{3.61}$$

This set of seven equations has finally seven possible unknown values, depending on the model employed for simulating the bus, as will be explained. [24] The problem can be solved in a typical iterative process, where the following increments have to be calculated:

$$\Delta x = J^{-1} \Delta f \tag{3.62}$$

where the incremental variables are

$$\Delta f = \Delta \left(f_1 f_2 ... f_7 \right)^T \tag{3.63}$$

$$\Delta x = \Delta (V_r \varphi_r I_r \phi_r I_s \phi_s s)^T \tag{3.64}$$

and the Jacobian matrix given in (3.65) contains the partial derivatives of the functions given in (3.54)–(3.61) with respect to the variables of x in (3.64):

$$J = \begin{pmatrix} \frac{\partial f_1}{\partial V_r} & \frac{\partial f_1}{\partial \varphi_r} & \cdot & \cdot & \cdot & \frac{\partial f_1}{\partial s} \\ \frac{\partial f_2}{\partial V_r} & \frac{\partial f_2}{\partial \varphi_r} & \cdot & \cdot & \cdot & \frac{\partial f_2}{\partial s} \\ \cdot & \cdot & \cdot & & & \cdot \\ \cdot & \cdot & & \cdot & & \cdot \\ \cdot & \cdot & & & \cdot & \cdot \\ \frac{\partial f_7}{\partial V_r} & \frac{\partial f_7}{\partial \varphi_r} & \cdot & \cdot & \cdot & \frac{\partial f_7}{\partial s} \end{pmatrix} \tag{3.65}$$

As the method given in (3.62)–(3.65) constitutes a classical NR algorithm, the values of Δx have to be initialized. Several tests have been carried out and our experience tells as that a good set of initial values can be (0.1 0.1 1.0 0.1 1.0 0.1 0) ^{T}, with angles in rad, and rms values in pu. As for error measurement, let us say that the functions f_1, f2 … f_7, must converge to 0, so the degree of approximation depends on the degree of accuracy desired from the calculation, which is obvious. Depending on initial values and desired degree of accuracy, iterations can vary but the iterative method runs fast enough not to constitute a

computational problem. Once the equations and the method have been presented, the following explanation has the goal of clearing up how these equations can be inserted in a load flow analysis program, which is explained in next section.[24]

3.8.1 PQ BUS MODEL

If the bus is modeled as a one, the complete process can be carried out in two steps, as illustrated in Fig. 3.13

1) ***Step 1****:* A load flow analysis is run to obtain V_s and φ_s , assuming P and Q to be known.

2) ***Step 2****:* The set of (3.54)–(3.61) is solved, with the unknown values given in (3.64).

3) Observations: The solution to (3.54)–(3.61) can be obtained by means of an iterative process, such as Newton Raphson method. The final result will be the machine steady-state operating point. Summarizing, and are input data, and stator and rotor currents and rotor voltage are the result, together with the value of slip. The value of the variable called mechanical power can be obtained by means of eq. 3.51.

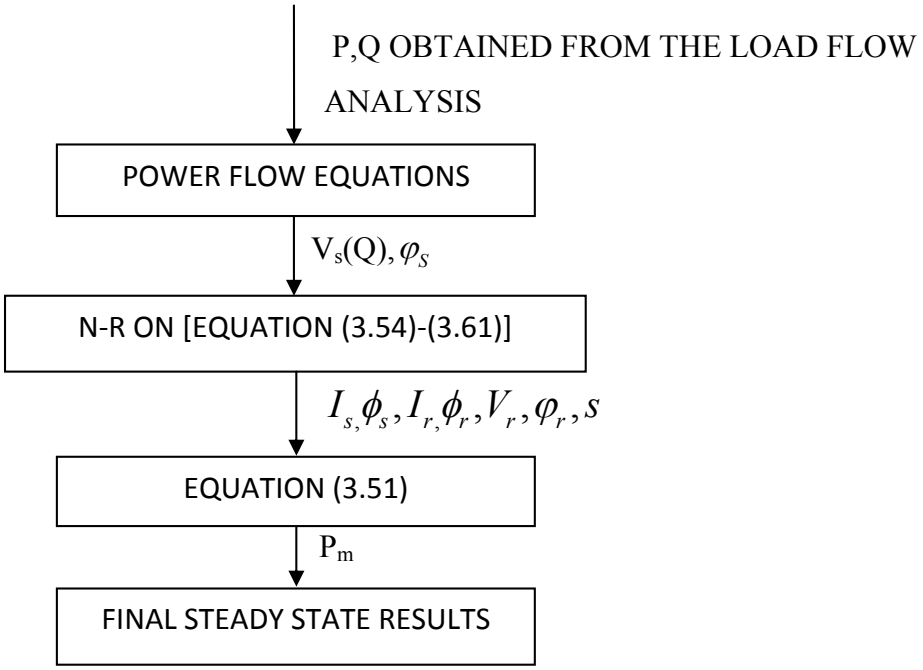

Figure 3.13 Steady state calculation procedure [24]

CHAPTER-4

RESULTS AND DISCUSSION

4.1 GENERAL

The analysis of steady state performance of DFIG, as mentioned in the algorithm, has been done in two steps. Firstly a load flow has been carried out by treating the bus to which DFIG is connected as PQ bus. For this the generation level of DFIG is assumed to be fixed. With the convergence of load flow, the bus voltage and bus voltage angle are calculated. Stator voltage V_s and stator voltage angle φ_s are bus voltage and bus voltage angle of the bus to which DFIG is connected. The analysis is carried out on a 4-bus system whereas, the DFIG parameters are taken from [25]. The bus data and line data for this 4-bus system is represented in Table 4.1(a) and 4.1(b).The DFIG parameters have been listed in table 4.2.

Table 4.1(a) Bus Data for 4-bus system

Bus	Bus Type	Voltage Specified	Gen. MW	Gen. MVAR	Load MW	Load MVAR	Qmin	Qmax
1	1	1.05	0	0	0	0	0	0
2	3	1	0	0	45	15	0	0
3	3	1	0	0	51	25	0	0
4	3	1	0	0	60	30	0	0

Table 4.1(b) Line Data for 4-bus system

Start Bus	End bus	R(pu)	X(pu)	1/2B(pu)	Tap Set Value
1	2	0.08	0.2	0	0
1	4	0.05	0.1	0	0
2	3	0.04	0.12	0	0
3	4	0.04	0.15	0	0

Table 4.2 DFIG Parameters

Stator Resistance, R_s	0.01
Stator Reactance, X_s	0.04
Rotor Resistance, R_r	0.01
Rotor Reactance, X_r	0.05
Mutual Reactance, X_m	2.9

Table 4.3 Steady state operating condition of DFIG with unity power factor (pf=1)

Pgi(pu)	Pm(pu)	Ps(pu)	Pr(pu)	s(pu)	Vs(pu)	Is(pu)	Vr(pu)	Ir(pu)
0.1	0.103	0.285	-0.182	0.529	0.954	0.299	-1.128	-0.475
0.2	0.204	0.349	-0.145	0.409	0.959	0.364	0.946	0.523
0.3	0.305	0.422	-0.117	0.324	0.963	0.438	0.817	-0.58
0.4	0.407	0.5	-0.093	0.257	0.968	0.516	-0.702	-0.643
0.5	0.509	0.58	-0.071	0.199	0.972	0.596	-0.588	-0.709
0.6	0.611	0.661	-0.05	0.149	0.977	0.677	-0.473	-0.778
0.7	0.713	0.744	-0.031	0.104	0.981	0.759	-0.352	-0.85
0.8	0.816	0.83	-0.014	0.063	0.985	0.842	0.227	-0.923
0.9	0.919	0.918	0.001	0.025	0.989	0.928	-0.096	-1
1	1.022	1.009	0.013	-0.011	0.993	1.016	0.044	-1.079
1.1	1.126	1.104	0.022	-0.044	0.997	1.107	0.188	-1.163
1.2	1.23	1.204	0.026	-0.075	1.001	1.203	-0.341	-1.251

Table 4.4 Steady state operating condition of DFIG at 0.95 leading power factor (generating both real and reactive power)

Pgi(pu)	Qgi(pu)	Pm(pu)	Ps(pu)	Pr(pu)	s(pu)	Vs(pu)	Is(pu)	Vr(pu)	Ir(pu)
0.1	0.033	0.104	0.356	-0.252	0.527	0.957	0.372	-1.28	0.554
0.2	0.066	0.207	-0.471	0.678	0.407	0.965	-0.488	1.157	0.664
0.3	0.099	0.31	0.582	-0.272	0.321	0.972	0.599	1.043	-0.769
0.4	0.131	0.412	0.682	-0.269	0.253	0.98	0.696	0.914	-0.864
0.5	0.164	0.515	0.769	-0.254	0.196	0.987	0.779	-0.77	-0.946
0.6	0.197	0.618	0.844	-0.226	0.146	0.994	0.849	-0.613	-1.016
0.7	0.23	0.72	0.907	-0.187	0.101	1.001	0.906	0.45	-1.075
0.8	0.263	0.822	0.961	-0.139	0.06	1.008	0.953	0.283	-1.124
0.9	0.296	0.923	1.005	-0.082	0.023	1.015	0.991	0.115	-1.164
1	0.329	1.025	1.042	-0.017	-0.012	1.021	1.02	0.054	-1.197
1.1	0.362	1.126	1.071	0.054	-0.044	1.028	1.043	-0.217	-1.223
1.2	0.394	1.227	1.095	0.131	-0.074	1.034	1.059	0.378	-1.244

Table 4.5 Steady state operating condition of DFIG at 0.95 lagging power factor (real power generated, reactive VAR demanded)

Pgi(pu)	Qgi(pu)	Pm(pu)	Ps(pu)	Pr(pu)	s(pu)	Vs(pu)	Is(pu)	Vr(pu)	Ir(pu)
0.1	-0.033	0.102	0.231	-0.129	0.531	0.951	0.243	-0.999	-0.407
0.2	-0.066	0.202	-0.273	0.475	0.411	0.952	-0.286	0.777	-0.408
0.3	-0.099	0.303	-0.336	0.639	0.326	0.954	-0.352	-0.637	0.432
0.4	-0.131	0.404	0.412	-0.008	0.258	0.956	0.431	-0.528	-0.476
0.5	-0.164	0.506	0.498	0.007	0.201	0.957	0.52	-0.433	-0.537
0.6	-0.197	0.608	0.593	0.015	0.15	0.959	0.618	-0.344	-0.612
0.7	-0.23	0.71	0.696	0.014	0.105	0.96	0.725	0.256	-0.702
0.8	-0.263	0.814	0.81	0.004	0.063	0.961	0.842	0.165	-0.805
0.9	-0.296	0.918	0.935	-0.017	0.025	0.962	0.972	-0.069	-0.924
1	-0.329	1.024	1.075	-0.052	-0.011	0.963	1.116	-0.04	-1.06
1.1	-0.362	1.131	1.234	-0.103	-0.045	0.964	1.28	0.159	-1.218
1.2	-0.394	1.241	1.419	-0.178	-0.078	0.965	1.471	-0.299	-1.404

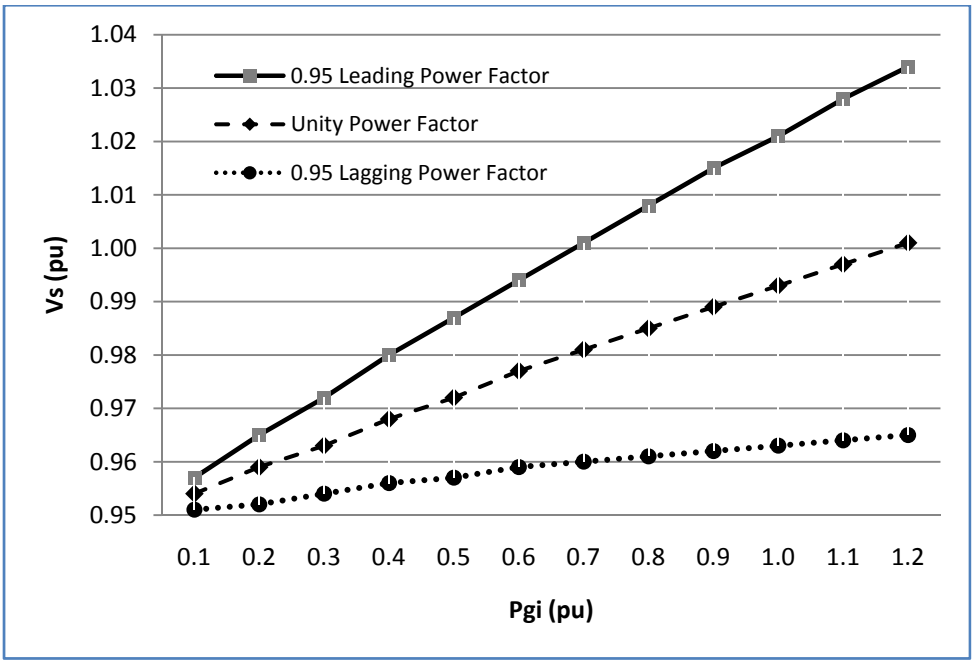

Figure 4.1 Graphical representation of stator current (Is) w.r.t generated power (Pgi)) for unity PF and 0.95 lagging and leading PF.

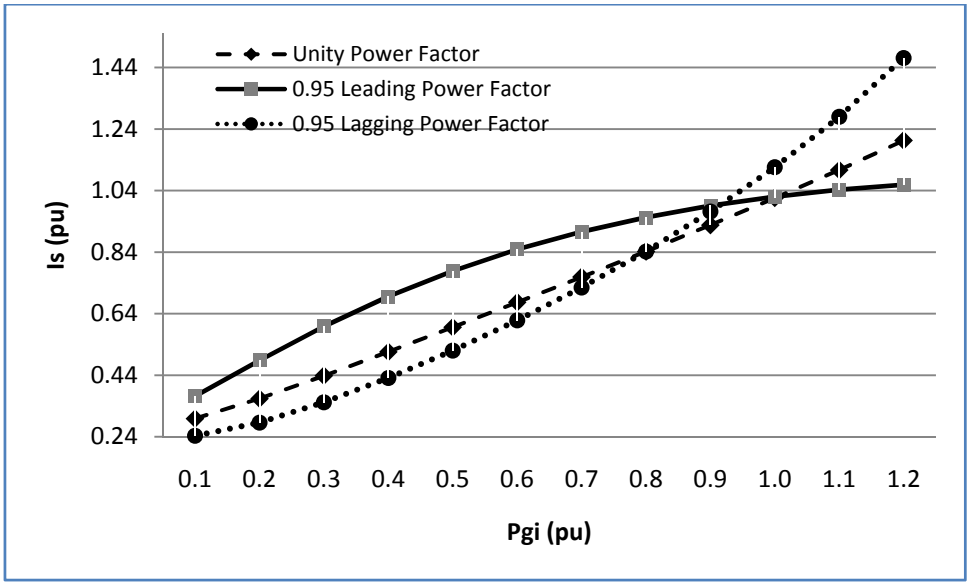

Figure 4.2 Graphical representation of stator current (Is) w.r.t generated power (Pgi) for unity PF and 0.95 lagging and leading PF.

Table 4.6 Steady state operating condition of DFIG at 0.85 leading power factor (both real and reactive powers are generated)

Pgi(pu)	Qgi(pu)	Pm(pu)	Ps(pu)	Pr(pu)	s(pu)	Vs(pu)	Is(pu)	Vr(pu)	Ir(pu)
0.1	0.062	0.106	0.435	-0.328	0.525	0.959	0.453	1.435	0.636
0.2	0.124	0.211	-0.621	0.832	0.403	0.97	-0.641	1.385	0.82
0.3	0.186	0.316	0.786	-0.47	0.317	0.98	0.802	1.287	0.983
0.4	0.248	0.421	0.916	-0.496	0.248	0.99	0.926	-1.135	1.111
0.5	0.31	0.525	1.012	-0.487	0.191	0.999	1.012	0.947	-1.204
0.6	0.372	0.627	1.076	-0.449	0.141	1.009	1.067	-0.741	1.268
0.7	0.434	0.729	1.116	-0.387	0.097	1.018	1.097	0.53	-1.309
0.8	0.496	0.83	1.138	-0.308	0.057	1.027	1.108	0.323	-1.333
0.9	0.558	0.93	1.145	-0.215	0.021	1.036	1.105	0.123	-1.345
1	0.62	1.03	1.143	-0.113	-0.013	1.045	1.094	0.068	-1.349
1.1	0.682	1.13	1.135	-0.005	-0.045	1.053	1.078	0.246	-1.35
1.2	0.744	1.229	1.125	0.105	-0.075	1.061	1.06	-0.411	1.349

Table 4.7 Steady state operating condition of DFIG at 0.85 lagging power factor (real power generated and reactive VAR demanded)

Pgi(pu)	Qgi(pu)	Pm(pu)	Ps(pu)	Pr(pu)	s(pu)	Vs(pu)	Is(pu)	Vr(pu)	Ir(pu)
0.1	-0.062	0.102	0.199	-0.097	0.532	0.948	0.21	-0.901	-0.354
0.2	-0.124	0.202	-0.245	0.447	0.412	0.947	-0.259	-0.655	0.323
0.3	-0.186	0.302	0.323	-0.02	0.327	0.946	0.341	0.509	-0.333
0.4	-0.248	0.403	0.416	-0.012	0.259	0.945	0.44	0.404	-0.381
0.5	-0.31	0.505	0.519	-0.014	0.201	0.944	0.55	-0.32	-0.458
0.6	-0.372	0.608	0.632	-0.025	0.15	0.942	0.671	0.246	-0.559
0.7	-0.434	0.711	0.756	-0.045	0.104	0.94	0.803	0.177	-0.678
0.8	-0.496	0.816	0.89	-0.075	0.063	0.939	0.949	-0.11	-0.814
0.9	-0.558	0.922	1.039	-0.118	0.024	0.937	1.11	0.041	-0.971
1	-0.620	1.03	1.208	-0.178	-0.013	0.935	1.292	0.038	-1.151
1.1	-0.682	1.141	1.404	-0.263	-0.049	0.933	1.505	0.129	-1.365
1.2	-0.721	1.342	1.623	-0.321	-0.056	0.956	1.672	0.235	-1.532

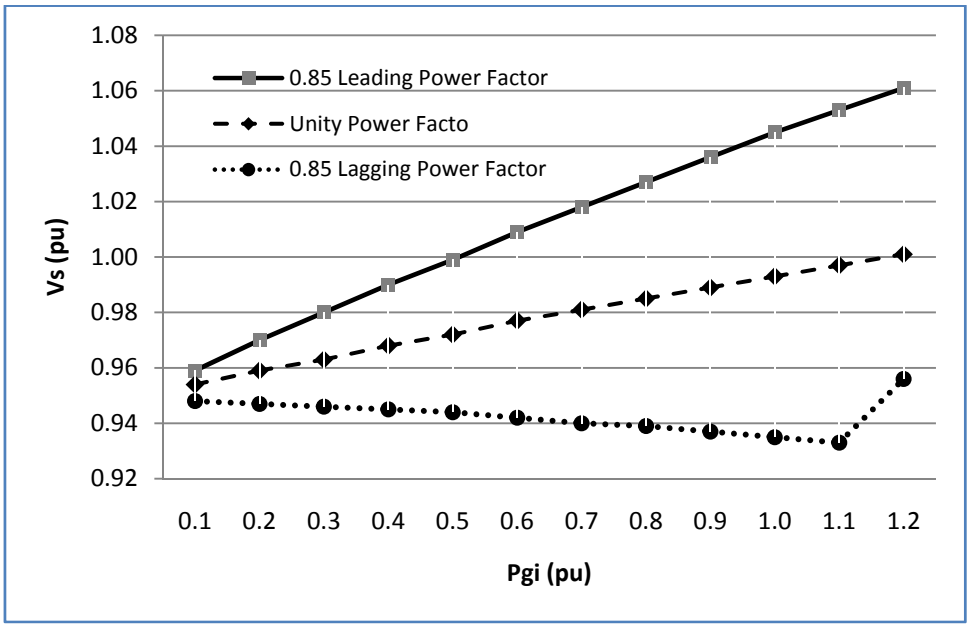

Figure 4.3 Graphical representation of stator current (Is) w.r.t generated power (Pgi)) for unity PF and 0.85 lagging and leading PF.

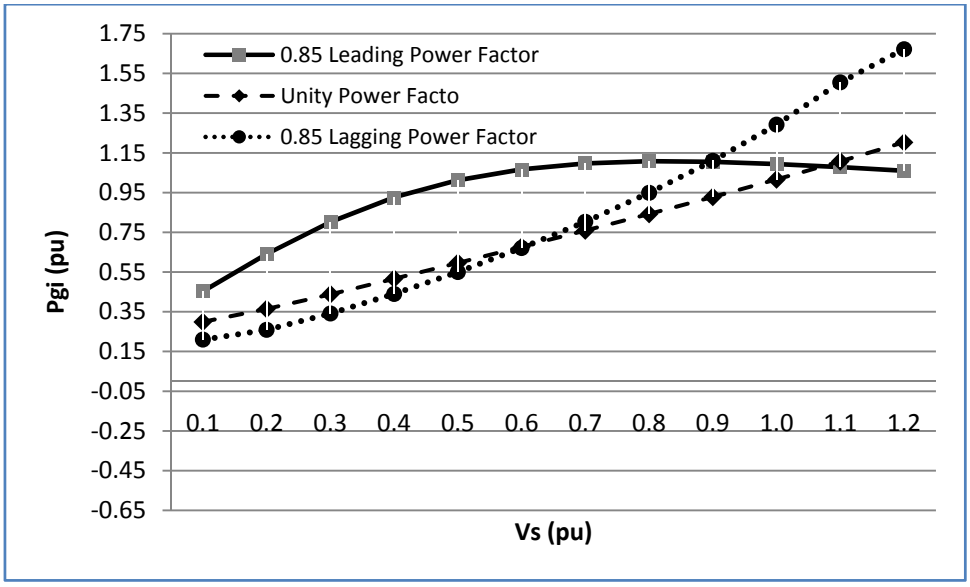

Figure 4.4 Graphical representation of stator current (Is) w.r.t generated power (Pgi) for unity PF and 0.85 lagging and leading PF.

4.2 DISCUSSION OF STEADY STATE PERFORMANCE OF DFIG

Generated power P_g is varied between 0.1 to 1.2 in step of 0.1 pu and the results are summarized in Table 4.3,4.4,4.5,4.6 and 4.7 respectively for unity, 0.95 (lagging and leading) and 0.85 (lagging and leading) power factors. It is observed that the stator output is always positive comprising the generator mode operation. The rotor power nature is varying for upto 0.8 pu, the P_r is negative and slip is positive. The magnitude of P_r decreases continuously and slips also decreases. After attaining minimum value of P_r, for higher value of P_g, both P_s and P_r assumes positive values and results into negative value of slip. With increase in P_g, the P_s increases and so the magnitude of rotor current also increase with increase in P_g. The rotor voltage magnitude decreases when P_g increases. After attaining the minimum value about rated 1.0 of P_g, the rotor voltage starts increasing.

The stator voltage increases for the leading power factor operation of DFIG and the stator voltage decreases for lagging power factor operation of DFIG. This trend is also shown in Figure 4.1 as a comparison to unity power factor.

For leading power factor operation, the slip decreases for initial values of P_g and after attaining a minimum positive value at 0.9 pu value of P_g, the slip start attaining higher

negative value. The stator and rotor current has the same trend as obtained for unity power factor operation i.e their values increases with increase in $P_{g.}$

For lagging power factor similar trends are obtained, however the stator current value increase significantly in comparison to respective value at leading power factor operation. This is shown in Figure 4.2.

For some typically lower values of P_g, P_s is showing positive values. However the generator output is positive and decided by the outputs of both stator and rotor.

The results at 0.85 leading and lagging power factor are presented in table 4.6 and 4.7 respectively. It is observed from the figure 4.3 and figure 4.4 that these are having the similar trends as obtained with 0.95 power factor operation. However, the higher I_s restricts its operation at lagging power factor.

CHAPTER-5

CONCLUSION AND FUTURE SCOPE

5.1 CONCLUSION

The steady state operation of DFIG connected to power system has been analyzed. The analysis is carried out on 4-bus system and one DFIG. The operation in leading power factor, lagging power factor and unity power factor made has been investigated. The following conclusions are drawn from the study:

- Stator current increases with the increase in real power generated. The stator current is high for lagging power factor operation in comparison to the respective output at leading power factor. Higher stator current at lagging power factor restricts its operation for high power outputs.
- For lower power generation slip is positive and for higher power generation slip becomes negative.
- The stator voltage is decided by the power system for leading power factor operation, voltage is more whereas for lagging power factor operation the stator voltage is less. The magnitude of rotor voltage is high at lower value of P_g which decrease with increase in P_g . After attaining a minimum value, it stats increasing.

5.2 SCOPE FOR FUTURE WORK

In this the steady state analysis of DGIG connected to power system is carried out. At the completion of this work. The scope is identified in the area of variable speed DFIG based wind turbine system as:

- Interaction of the DFIG wind turbine system with more realistic grid models. The grid may have other generators harnessing various renewable resources.
- Evaluating the performance by taking wind speed as input parameter.

REFERENCES

1. De Haan,; S.W.H. Polinder, ; H. Kling, W.L. "General model for representing variable speed wind turbines in power system dynamics simulations," *IEEE Transactions on power Systems,* Volume: 18 pp. 144 – 15, Feb 2003.
2. Mustafa; Milanovic ; Jovica V. "DFIG modeling and the relevance of model simplification," *8th International Conference and Exhibition on Electricity Distribution,* CIRED 2005,pp. 1 – 5, June 2005.
3. Ekanayake, J.B. ;Holdsworth, L ;Wu, X. ; Jenkins, N., "Dynamic modeling of Doubly Fed Induction generator wind turbines," *IEEE Transactions on Power Systems,* Volume: 18 , Issue: 2, pp. 803 – 809, May 2003.
4. Mohseni, M.; slaman, S. "An improved modeling and control approach for DFIG-based wind generation systems," *Power Engineering Conference, 2009.AUPEC 2009. Australasian Universities,*pp. 1 – 6, 27-30 Sept. 2009.
5. Cheng, K.W.E. Lin, J.K. ; Bao, Y.J. ; Xue, X.D. "Review of the wind energy generating system,"*8th International Conference on Advances in Power System Control, Operation and Management (APSCOM 2009),* pp. 1 – 7, 8-11 Nov. 2009.
6. YazhouLei; Mullane, A. ; Lightbody, G. ; Yacamini, R. "Modeling of the wind turbine with a doubly fed induction generator for grid integration studies," *IEEE Transactions on Energy Conversion,*Volume: 21 , Issue: 1 ,March 2006.
7. HyongSik Kim and Dylan Dah-Chuan Lu, "Wind Energy Conversion System from Electrical Perspective - A Survey," *Smart Grid and Renewable Energy*, vol. 1, no. 3, pp.119-131, Nov. 2010.
8. Francoise Mei, "Small Signal Modeling and Analysis of Doubly Fed Induction Generator in Wind Power Applications," *Ph.D. dissertation*, Control and Power Group Dept of Electrical and Electronic Engineering Imperial College London University of London.
9. K. C. Divya and P. S. N. Rao, "Models for wind turbine generating systems and their application in load flow studies," *Elect. Power Syst. Res.,* vol. 76, pp. 884–856, 2006.
10. Q. Wang and L. Chang, "An intelligent maximum power extraction algorithm for inverter-based variable speed wind turbine systems," *IEEE Trans. Power Electronics*, vol. 19, no. 5, pp. 1242-1249, Sept. 2004.

11. Raymond W. Flumerfelt and Su Su Wang, “Wind turbines,” in Access Science, McGraw-Hill Companies, 2009, [Online]. Available: http://www.accessscience.com.
12. Global wind energy council, “global wind energy report,” *GWEC annual energy market update 2010*. [online]
13. Chitti Babu B., ; Mohanty, K.B. “Converter performance of grid connected wind power generating systems,” 5th IET International Conference on Power Electronics, Machines and Drives (PEMD 2010), pp. 1 – 6, 19-21 April 2010.
14. Blecharz, K. ;Krzeminski, Z. ; Bogalecka, E. “Control of a doubly-fed induction generator in wind park during and after line-voltage distortion,” 8th International Symposium on Advanced Electromechanical Motion Systems & Electric Drives Joint Symposium, ELECTROMOTION 2009. pp. 1 – 6, July 2009.
15. Tapia, A.; Tapia, G.; Ostolaza, J.X. ; Saenz, J.R. “Modeling and control of a wind turbine driven doubly fed induction generator,” IEEE Transactions on Energy Conversion, Volume: 18, Issue: 2, pp. 194 – 204, June 2003.
16. Das, M.K.; Chowdhury, S. ; Chowdhury, S.P. ; Gaunt, C.T. “Control of a grid connected doubly-fed induction generators for wind energy conversion,” Proceedings of the 44th International Universities Power Engineering Conference (UPEC), 2009,pp. 1 - 5 , Sept. 2009.
17. Aktarujjaman, M.; Haque, M.E. ; Muttaqi, K.M. ; Negnevitsky, M. ; Ledwich, G. “Control Dynamics of a doubly fed induction generator under sub- and super-synchronous modes of operation,” 2008 IEEE Power and Energy Society General Meeting - Conversion and Delivery of Electrical Energy in the 21st Century, July 2008
18. Richard Gagnon; Gilbert Sybille; Serge Bernard; Daniel Paré; Silvano Casoria; Christian Larose
19. “Modeling and Real-Time Simulation of a Doubly-Fed Induction Generator Driven by a Wind Turbine,” *Presented at the International Conference on Power Systems Transients (IPST’05) in Montreal, Canada,* Paper No. IPST05-162, June 19-23, 2005.
20. The MathWorks, “SimPowerSystems For Use with Simulink”

21. R. Pena ; J. C. Clare ; and G. M. Asher, “Doubly fed induction generator using back-to-back PWM converters and its application to variable-speed wind-energy generation,” *IEE Proc. Elect. Power Appl.*, vol. 143, no. 3, pp. 231-241, 1996.
22. Petersson ; T. Thiringer ; L. Harnefors and T. Petru, “Modeling and experimental verification of grid interaction of a DFIG wind turbine,” *IEEE Trans. Energy Convers.*, vol. 20, no. 4, pp. 878–886, Dec. 2005.
23. B.H. Chowdhury and S. Chellapilla, “Double-fed induction generator control for variable speed wind power generation,” *Electric Power Systems Research*, vol. 76, iss. 9-10, pp. 786-800, June 2006.
24. Jose Fernando, Medina Padron and Elias Feijoo Lorenzo, *“Calculating steady-state operating condition for doubly-fed induction generator wind turbines,”* IEEE transaction on power system, vol.25, no. 2, May 2012
25. J.S. Dillon and D.P. Kothari, “Power system optimization,” Preintce Hall of India Private Limited.